

85-981-14195

**GEOLOGICAL BRANCH
ASSESSMENT REPORT**

14,195

INTERPRETATION REPORT

10/86

INPUT MK VI ELECTROMAGNETIC/MAGNETIC SURVEY

OMNI RESOURCES INCORPORATED

ADAMS LAKE AREA

FILMED

PROJECT # 27H17

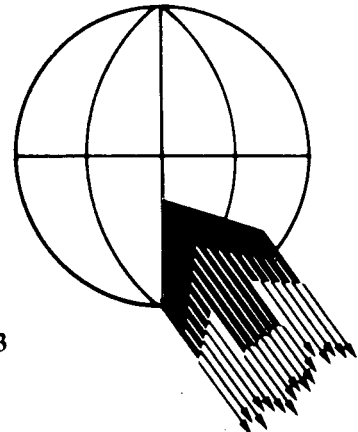
JUNE 1985

Kanloops M.D.

82 M 4

51° 10'

119° 44'



C O N T E N T S

1.	INTRODUCTION	1
2.	PROJECT LOCATION	2
3.	SURVEY OPERATIONS	2
	3a. Survey Personnel	2
	3b. Instruments	3
	3c. Production	4
	3d. Products	4
	3e. Survey Procedure	5
	3f. Magnetic Diurnal	6
4.	DATA COMPILATION	7
	4a. Data Recovery	7
	4b. Computer Processing	9
5.	INPUT DATA PRESENTATION	10
6.	INTERPRETATION - GENERAL	12
	6a. Geological Perspective	12
	6b. Conductivity Analysis	14
7.	INPUT INTERPRETATION	17
8.	CONCLUSIONS AND RECOMMENDATIONS	22
	 <u>APPENDICES</u>	
	APPENDIX A BARRINGER/QUESTOR MARK VI INPUT ^(R) System	A-1
	APPENDIX B The Survey Aircraft	B-1
	APPENDIX C INPUT System Characteristics	C-1
	APPENDIX D INPUT Processing	D-1
	APPENDIX E INPUT Interpretation Procedures	E-1

Data Sheets

Listing of Flight Path Recovery Fiducial Points

1. INTRODUCTION

This report details the interpretation of a Helicopter-borne INPUT electromagnetic and magnetic survey for Omni Resources Incorporated (ORI). The system used was the Questor/Barringer MK VI, 2 ms, INPUT system. The standard specifications for the INPUT transmitter and receiver are outlined in Appendix A.

The interpretation was commissioned by Mr. Ernie Bergvinson of ORI on May 1, 1985. Philip Salib, Geophysicist of Questor, supervised the data compilation and interpretation of the area through to the completion of the project in June, 1985.

The survey objective is the detection and location of base metal sulphide conductors as well as any structures and conductivity patterns which could have a positive influence on base metal exploration.

The two survey areas consist of 66.9 kilometres of traverse and control lines. These were flown between June 24 and June 30, 1984 using Barriere as the survey operations base.

The total cost was \$ 9031.50

2. PROJECT LOCATION

The survey areas lie within the Province of British Columbia, approximately 10 kilometres north of Skwaam Bay on Adams Lake. The areas are located between latitudes $51^{\circ}06'$ and $51^{\circ}12'$ longitudes $119^{\circ}41'$ and $119^{\circ}047'$ (figure 1). Map sheet Adams Plateau (N.T.S. 82M/4) includes the survey site.

3. SURVEY OPERATIONS

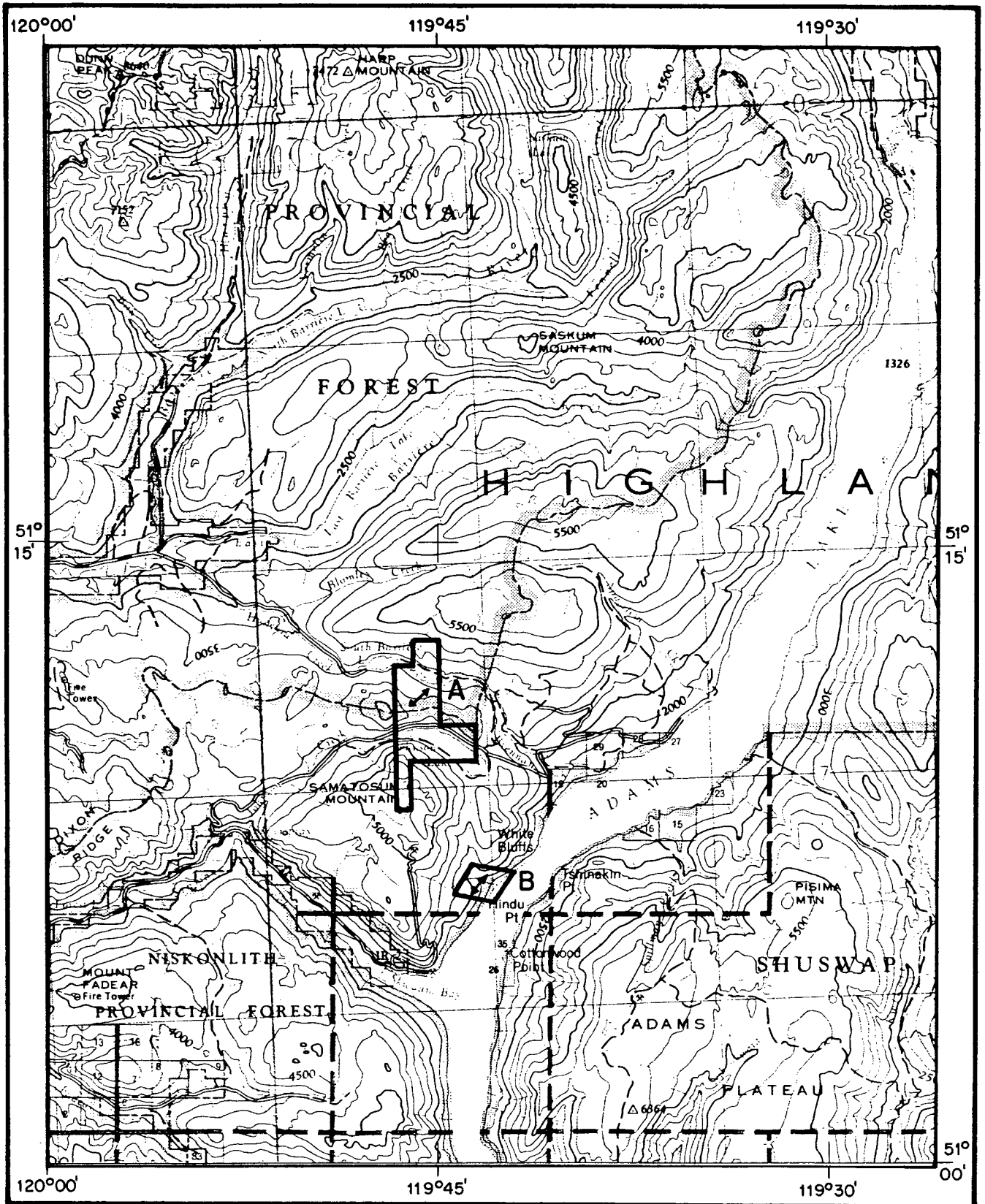
3a. Survey Personnel

The survey crew was made up of experienced Questor employees:

Crew Manager	- Dan Martyn
Pilot/Captain of Aircraft	- Bob Masson (Trans Canada)
Navigator	- Bill Smith
INPUT Equipment Technician	- Dan Makos
Aircraft Engineer	- John Caza (Trans Canada)

The flight path recovery was completed at the survey base, while the final data compilation and drafting was carried out by Questor at its Mississauga, Ontario office. The magnetic and electromagnetic processing was carried out using Questor software and computer drafted. The INPUT interpretation and reporting was completed by Philip Salib.

A preliminary compilation of results was presented to ORI after signing the contract.



SURVEY LOCATION MAP

Scale 1: 250 000

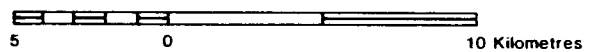


Figure 1

3b. Instruments

A Bell 205A Helicopter (registration C-GLMC owned and operated by Trans Canada) equipped with the following instruments was used for the survey:

1. Questor/Barringer Mark VI INPUT 2 msec. Electromagnetic System;
2. Geometrics G-803 Proton Magnetometer (1 gamma sensitivity);
3. Sonotek SDS 1200 Data Acquisition System;
4. RMS GR33 Analog Recorder;
5. 35mm Camera, Intervalometer and Fiducial System;
6. Sperry Radio Altimeter ($\pm 3\%$ accuracy);

The equipment, such as the INPUT system, magnetometer and radar altimeter were regularly calibrated at the beginning and end of each survey flight as well as in mid-flight, whenever necessary. Details of the calibration procedures are given in Appendix C.

The continuous chart speed of the RMS recorder was set at 15 cm./minute.

3c. Production

The flight line spacing over the block was 200 metres. Table 1 summarizes the kilometres flown during the survey operation.

Table 1

Block A	Traverse lines	55.2 km.
	Control lines	1.2 km.
Block B	Traverse lines	10.5 km.
	Total lines	66.9 km.

3d. Products

The following list are the products delivered by Questor to ORI with four copies of the report:

1. one sheet Chronaflex unscreened master orthophoto mosaic, scale 1:10,000;
2. one sheet master photo mosaic with electromagnetic and magnetometer information and interpretation shown thereon, scale 1:10,000;
3. one sheet magnetics overlay, scale 1:10,000;
4. four white prints of (2);
5. one copy computer generated analogue profiles at a scale of 1:10,000;
6. one set Applicon colour contoured magnetics for the Adams Plateau region @ 1:50,000 scale;
7. one set Applicon shadow relief colour contoured magnetics for the Adams Plateau region @ 1:50,000 scale;

8. anomaly data sheets;
9. listing of flight path recovery fiducial points.

3e. Survey Procedure

During the survey, the helicopter maintained a terrain clearance as close to 122 metres as possible, with the receiver coil (bird) at approximately 49 metres above the ground surface. In areas of substantial topographic relief and large population, the aircraft height may exceed 122 metres for safety reasons. The height of the bird above the ground is also influenced by the aircraft's air speed (see figure C1 in Appendix C), which was maintained at 40 to 60 knots, while on survey.

Whenever possible, the traverse lines were flown in alternate flight directions (e.g., north then south) to facilitate the interpretation of dipping conductors. When the traverse line spacing exceeded twice the normal spacing interval over a 3.2 kilometre distance, the gap is normally filled with an appropriately spaced fill-in line at a later date.

The details of each production flight are documented on the flight logs by the equipment technician. The logs include the survey times, line numbers and fiducial intervals, as well as a record of equipment irregularities and atmospheric conditions. One may refer to these logs in order to relate the flight path film to the geophysical data.

During the course of the survey the following data were recorded:

1. INPUT Electromagnetic results represented by six channels of successively increasing time delays after cessation of the exciting pulse (Appendix A);
2. a record of the terrain clearance as provided by radio altimeter;
3. a photographic record of the terrain passing below the aircraft as obtained from a 35 mm. camera;
4. time markers impressed synchronously on the photographic and geophysical records to facilitate accurate positioning on photomosaics;
5. airborne magnetometer data;
6. ground base station magnetometer data.

3f. Magnetic Diurnal

Diurnal variations in the earth's magnetic field had been recorded to an accuracy of ± 1 nT using a base station equipped with a Geometrics 826 Proton Precession Magnetometer. It was monitored periodically during the day for severe diurnal changes (magnetic storms). A variation of 100 nT over a 5 minute time period was considered to be a magnetic storm. During such an event, the survey would normally have been discontinued or postponed and the survey data would have been scrubbed.

4. DATA COMPILATION

4a. Data Recovery

The flight path of the aircraft is recorded by a frame camera on black and white, 125ASA, 35mm. film which is exposed continuously during flight at a rate of 1 frame every 2 seconds. The apperture setting on the camera can be manually adjusted by the operator during flight, assuring the proper exposure of the film. The camera is fitted with a wide angle 18 mm. lens.

The camera is controlled by the fiducial time system of the data acquisition system once every 2 seconds. Fiducial numbers are imprinted on the film, marked onto the analog records and recorded digitally at the same instant.

The flight line headings are opposite on adjacent lines, which are normally flown sequentially in an "S" pattern. The navigation references are flight strips at a scale of 1:20,000 which are made from the base maps. The equipment operator enters the flight details information into the digital data system which are recorded and verified (read-after-write). The information includes line number, time fiducial range and other pertinent flight information. This information is compared to the film, analog records and the magnetic base station recording at the completion of the survey flight.

The film and all records are developed, edited and checked at the completion of each flight. Recovery of the flight track is carried out by comparing the negative of the 35mm. film to the topographic features of the base map. Coincident features are picked and plotted on exact copies of the stable mosaic base map on

which the final results are drafted. Points are picked at an average interval of 1 kilometre. This corresponds to one whole fiducial unit or 20 seconds. The picked points will not necessarily fall on whole fiducial numbers, but on the final presentation, only the first and last whole fiducial numbers on a line are marked on each flight line. By interpolation, the whole numbers are marked as ticks along the flight path. This keeps the anomaly and interpretation maps free of unnecessary numbers.

These procedures are performed on the survey site daily by the crew manager so that the data quality and progress may be measured objectively. Reflights for covering navigational gaps and other deficiencies are usually flown on the following day.

The analog records are inspected for coherence with specifications, and anomalies are selected for classification and plotting. Selected anomalous conductors are positioned by plotting their fiducial positions, less the lag factor (Appendix C). These resultant positions are located by interpolating between fiducial points established by the flight path recovery process.

The survey results are presented as three products. There is an INPUT anomaly map with interpretation and a magnetic contour overlay. The following chapters describe the interpretation of INPUT results and present recommendations for ground follow-up surveys. A colour presentation of the magnetic contours and a "sun shadow" colour magnetic representation was also included as a standard product.

4b. Computer Processing

The completed flight path is accurately digitized on a flat-bed digitizer at Questor using the picked point co-ordinates. The recovery is then routinely verified by a computer programme 'speed check', which flags any abnormalities in the distance per fiducial unit between picked points on a traverse line. As a final check, the rough magnetic contour maps are examined for contour irregularities that could be attributed to recovery errors.

5. INPUT DATA PRESENTATION

The base maps for the survey area are ortho-photomosaics constructed from 1:55,000 air photographs supplied by British Columbia Ministry of Environment and taken in 1982. The photomosaic was used to construct the navigation flight strips and also the base onto which the flight path was recovered.

The INPUT anomaly map presents the information extracted from the analog records. This consists chiefly of the peak anomaly positions and response characteristics, surficial responses, up-dip responses, and magnetic anomaly locations. In effect, these represent the primary data analysis. The symbols are explained in the map legend, but the following observations are presented:

- position of peak anomaly;
- conductance or conductivity-thickness;
- amplitude of channel 2 response;
- position and peak amplitude of associated magnetic anomalies;
- where present, surficial, up-dip, poorly defined responses have been identified with a unique symbol.

The interpretation maps outline the geophysical-geological interpretation of the INPUT electromagnetic, magnetic, geological and physiographic data. Bedrock conductors have axis locations and dip directions, when they are interpretable. The anomalous zones which are recommended for follow-up have a reference label assigned, to which additional comments and recommendations are directed in the Interpretation Section this report. Surficial

response sources are mapped out by boundaries showing their interpreted lateral extent. The following list summarizes the interpretation presentation:

- bedrock conductor axis, probable and possible;
- conductor dip;
- surficial conductor outlines;
- anomalous conductors selected for ground evaluation with reference number.

6. INTERPRETATION - GENERAL

6a. Geological Perspective

Adams Lake area has been mapped in detail by V.A. Preto.

The regional geology of Adams Lake area shows that it is mainly formed of the Eagle Bay Formation (EBF) which is about 4,300 metres thick. This formation is thought to be of the Mississippian and older age. North to northwest of Johnson Creek the Eagle Bay Formation consists of a structurally lower and complexly folded sedimentary sequence of quartzite, calcareous siltstone, impure limestone and grey phyllite. This is interlayered with and structurally overlain to the northeast by a sequence of basic pillow lavas, breccias and tuffs which are folded.

In the area between Adams Lake and Johnson Creek, the structurally lowest Eagle Bay Formation rocks are highly sheared and intensely foliated pyritic and tuffs.

Folds are not evenly distributed but tend to occur in clusters that are generally limited lateral extent but are fairly continuous along strike.

Numerous base metal occurrences, many of which are stratabound massive sulphide deposits syngenetic with their host rocks.

References:

Preto, V.A.: "Barriere Lakes-Adams Plateau Area"; B.C. Ministry of Energy, Mines & Pet. Res., Geological Fieldwork 1978;

Preto, V.A. et al: "Barriere Lakes-Adams Plateau Area"; B.C. Ministry of Energy, Mines & Pet. Res., Geological Fieldwork 1979;

Preto, V.A.: "Barriere Lakes-Adams Plateau Area"; B.C. Ministry of Energy, Mines & Pet. Res., Geological Fieldwork 1980;

Schiarizza, P., et al: "Geology of the Adams Plateau-Clearwater Area"; B.C. Ministry of Energy, Mines & Pet. Res., Preliminary Map 56.

6b. Conductivity Analysis

The conductivity-thickness products of planar horizontal and thin, steeply dipping conductors are proportional to the time constant of the secondary field electromagnetic transient decay. This transient may be closely approximated by an exponential function for which the conductivity-thickness product (TCP) is inversely proportional to the log difference of two channel amplitudes at their respective sample times.

These response functions are presented in the form of graphs in which the amplitudes of the 6 channels of INPUT response are plotted on a logarithmic scale against conductivity. The relative amplitudes of the secondary response, at any given conductivity, may be accurately related to the depth of a conductor below the surface. These are typically referred to as Palacky nomograms. These are available for a number of conductor geometrics. It has been found that the shape of the decay transient and its amplitude is usually unique to a particular geometry. Therefore, if the origin of a conductive response is in question, a good "fit" of the peak response amplitude to one nomogram will define its origin.

The 90° nomogram was utilized exclusively to determine the apparent conductances of the responses obtained from the survey. This procedure is valid for near vertical conductors, within a dip range of $45-135^{\circ}$, relative to the aircraft flight direction.

Although the conductor depth can be interpreted from nomograms, the short strike lengths and the variability of conductor geometry may result in the over-estimation of depths.

The INPUT system depth capability is typically 200 metres for a vertical, 600 metre strike length by 300 metre depth extent target. The effective penetration depth increases for a dipping target and decreases for a smaller size conductor.

Depths were only determined for responses which appear to fit the interpretation model - a thin near vertical plate with a strike length of greater than 500 metres. Qualifications for these determinations are summarized in the interpretation section.

The depths for 5 and 6 channel anomalies were corrected for the interpreted conductor strike intersection relative to the flight line direction and the effects of aircraft altitude deviations from a flight altitude of 120 metres.

An anomaly listing at the back of this report summarizes each anomalous response in a numerical sequence. In addition to the standard anomaly parameters, an "anomaly type" classification has been added. The letters correlate with the plotted symbols according to the following table.

<u>ANOMALY TYPE</u>	<u>RESPONSE SOURCE</u>	<u>SYMBOL</u>
BLANK	bedrock conductors	circular
S	surficial (overburden or lakebottom) conductivity	diamond
U	up-dip accessory peak to main response	half circular, half diamond, symbolically "pointing" in dip direction
W	down-dip accessory peak to main response	half circular, half diamond, symbolically "pointing" in dip direction
P	poorly defined response	asterisk "*" in lower left quadrant
C	cultural source	square

The "P" poorly defined response may not yield signatures diagnostic of a discrete bedrock anomaly to standard electromagnetic prospecting equipment. Interpreted axis locations may be approximate for these intercepts.

7. INPUT INTERPRETATION

With the exception of the formational conductive bands, the area could be considered resistive. The major conductor bands have northwest to southwest trends which confirm the general magnetic trends. They also follow the schistosity trend. These conductors are dipping to the northeast. Their dip angle was not calculated due to absence of the leading peak information. High magnetic gradient trend is recognized southwest of South Barrier Lake and extends to the southeast through Johnson Lake.

Between flight lines 20232N and 20243S the responses are consistently high. These responses changed their characteristics suddenly from line 20252N and to the south of the survey area. This could be attributed to the presence of a structural fault that has a northeast-southwest trend parallel to the flight lines.

Some of our selection criteria are as follows:

- isolated horizon or offset from formational conductors;
- conductance increase;
- width improvement;
- structure (folding, faulting, dip change);
- magnetic correlation with increased conductance.

Four conductive zones were recommended for further ground follow-up. These zones are:

CONDUCTIVE ZONE 24G

Priority 2

BLOCK A

Line	20243S
Terrain clearance	131 m
Dip	northeast
Strike Intersection	45°W
Strike Length	>300 m
Conductance	18S
Depth	20 m
Magnetic Coincidence	-
Related Responses	20232G, 20243G

The conductive ZONE 24G is dipping to the northeast and is located on the northwest side of a possible fault plane. The width of the responses are, in part, derived from the oblique intersection of the flight lines with the conductor. Meanwhile, the 24G transient response has a perfect match to a sheetlike conductor geometry.

CONDUCTIVE ZONE 35W

Priority 1

BLOCK A

Line	20351S
Terrain Clearance	116 m
Dip	?
Strike Intersection	45°W
Strike Length	300 m
Conductance	8S
Depth	?
Magnetic Coincidence	-
Related Responses	20341T, 20351W, 20351T, 20352A.

The conductor ZONE 35W has a deep transient response characteristic. It is located on the west side of a high gradient magnetic feature. The response transient does not fit a dipping sheet nomogram; especially the latter channels have a rapid decay rate. A complex high conductance source geometry may be anticipated; a favourable criterion for sulphide concentrations.

CONDUCTIVE ZONE 40C

Priority 2

BLOCK A

Line	20402N
Terrain Clearance	119 m
Dip	?
Strike Length	>100 m
Conductance	4S
Depth	?
Magnetic Coincidence	-
Related Responses	20402C

The 40C intercept has four channel transient decay which left the quantitative interpretation risky. Visually, the profile has a good decay characteristic, however, the low amplitude early channel deflections are affected by surficial responses with background noise disturbing the later channels.

CONDUCTIVE ZONE 67H

Priority 2

BLOCK B

Line	20670S
Terrain Clearance	129 m
Dip	NE
Strike Intersection	90°
Strike Length	+ 700 m
Conductance	17S
Depth	50-60 m
Magnetic Coincidence	-
Related Responses	20660P, 20670H

This conductor lies on the flank of a small high magnetic peak. It is parallel to the schistosity in this area. Its conductance and good INPUT transient decay recommend it for further ground follow-up studies.

8. CONCLUSIONS AND RECOMMENDATIONS

The combined INPUT/magnetic survey in Adams Lake has resulted in the delineation of many conductive targets which fit the standard criterion for base metal sulphide conductors. Depths for the selected targets fall within a range of 20-80 metres.

The following list summarizes our selection of conductive anomalies for immediate consideration.

<u>Priority 1</u>	<u>Priority 2</u>
35W	24G
	40C
—	<u>67H</u>
1	3

First priority conductors have good geophysical characteristics, as well as a "favourable" geological environment. Second priority zones may be prominent in either of the above criterion.

Other conductors exist in the survey area and their axes presented on the interpretation map. These should also be examined where geological environment is favourable.

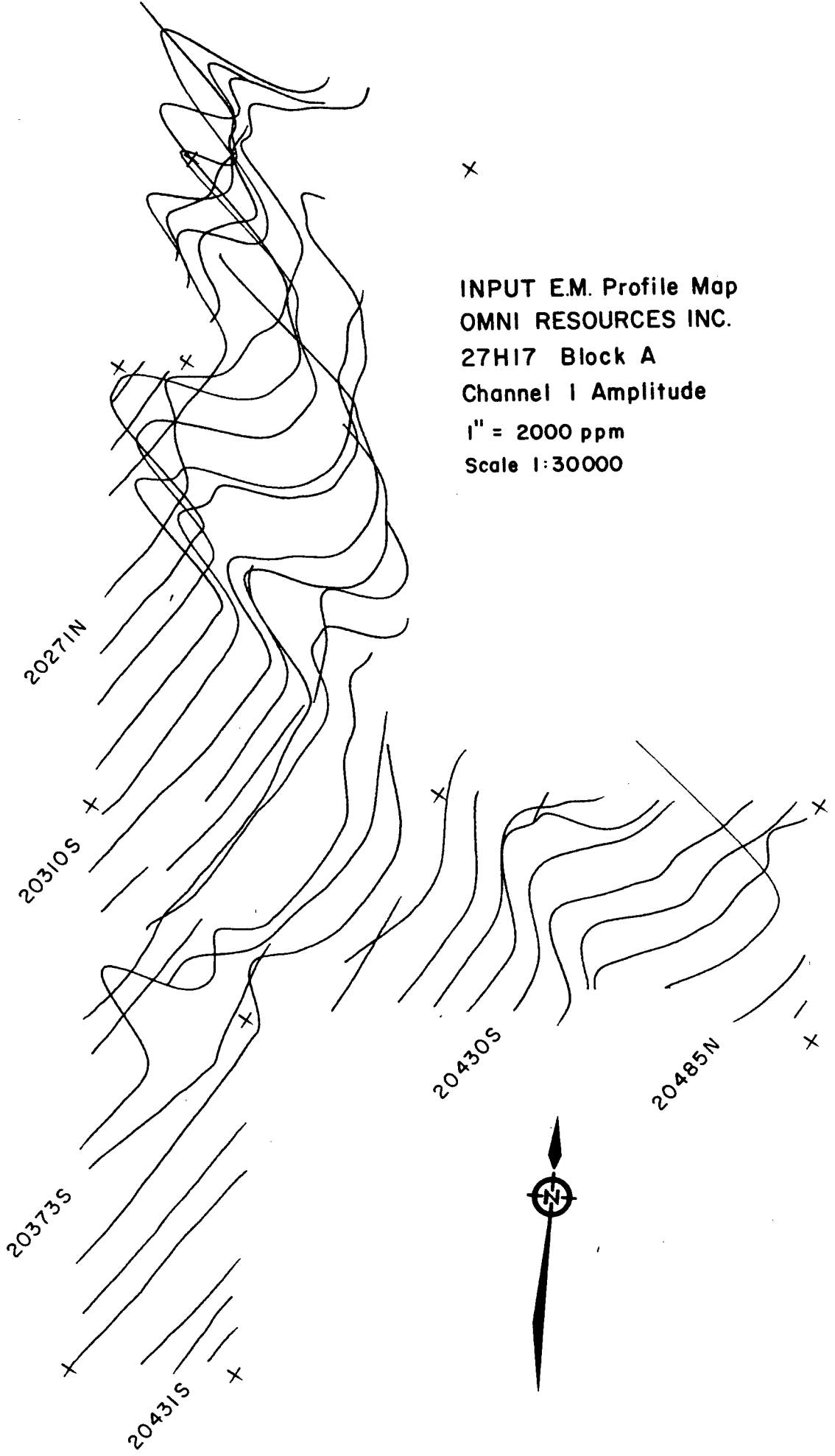
Respectfully submitted,
QUESTOR SURVEYS LIMITED,



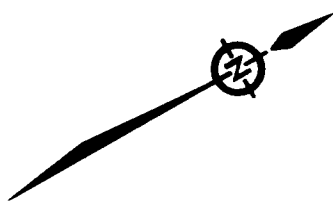
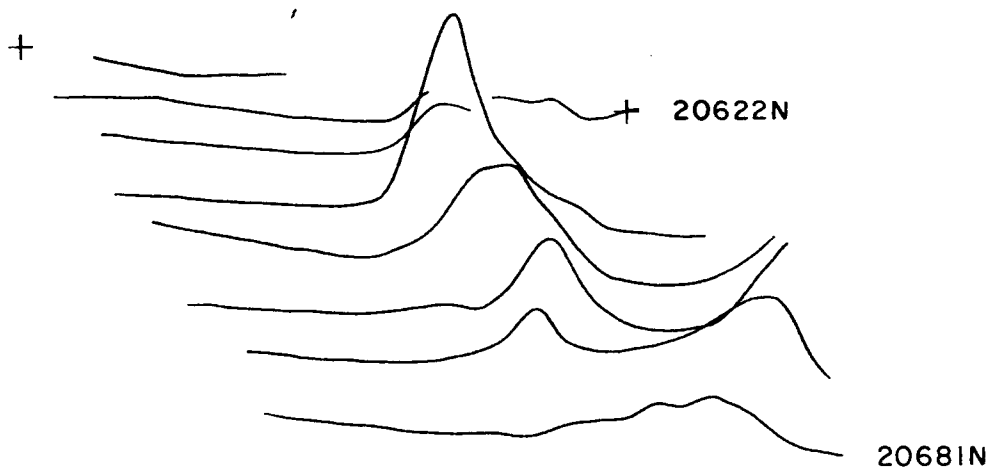
Philip Salib,
Geophysicist.

x

INPUT E.M. Profile Map
OMNI RESOURCES INC.
27H17 Block A
Channel 1 Amplitude
1" = 2000 ppm
Scale 1:30000



INPUT E.M. Profile Map
OMNI RESOURCES INC.
27H17 Block B
Channel 1 Amplitude
1" = 2000 ppm
Scale 1:30000



APPENDIX ABARRINGER/QUESTOR MARK VI INPUT^(R) Helicopter System

The INDUCED Pulse Transient (INPUT) method is a system whereby measurements are made, in the time domain, of a secondary electromagnetic field while the primary field is between pulses. Currents are induced into the ground by means of a pulsed primary electromagnetic field which is generated from a transmitting loop around the helicopter. By using half-sine wave current pulses (Figure A-1) and a transmitter loop of large turns-area, a high signal-to-noise ratio and the high output power needed for deep penetration, are achieved.

Induced current in a conductor produces a secondary electromagnetic field which is detected and measured after the termination of each primary pulse. Detection of the secondary field is accomplished by means of a receiving coil, wound on an air core form, mounted in a PCV plastic shell called a "bird" and towed behind and below the helicopter on 76 metres (250 feet) of coaxial cable. The received signal is processed and recorded by equipment within the helicopter.

The axis of the receiving coil may be vertical or horizontal relative to the flight direction. In rolling or hilly terrain the standard or horizontal coil axis is preferred, although in steep terrain, the vertical axis coil optimizes coupling with horizontal or dipping stratigraphy. The secondary field is in the form of a decaying voltage transient, measured in time, at the termination of the primary transmitted pulse. The amplitude of the transient is proportional to the amount of

current induced into the conductor, the conductor dimensions, conductivity and the depth beneath the helicopter.

The rate of decay of the transient is inversely proportional to conductance. By sampling the decay curve at six different time intervals and recording the amplitude of each sample, an estimate of the relative conductance can be obtained. Transients due to strong conductors such as sulphides and graphite, usually exhibit long decay curves and are therefore commonly recorded on all six channels. Sheet-like surface conductive materials, on the other hand, have short decay curves and will normally only show a response in the first two or three channels.

For homogeneous conditions, the transient decay will be exponential and the time constant of decay is equal to the time difference at two successive sampling points divided by the log ratio of the amplitudes at this point.

TRANSMITTER SPECIFICATIONS

Pulse Repetition Rate	211	per sec
Pulse	Half sine	
Pulse Width	2.0	millisec
Off Time	2.7	millisec
Output Voltage	60	volts
Output Current Peak	235	amperes
Output Current RMS	106	amperes
Output Current Average	60	amperes
Coil Area	167 m. ²	(1,800 ft. ²)
Coil Turns	6	
Electromagnetic Field Strength (peak)	233,800	amp-turn-meter ²

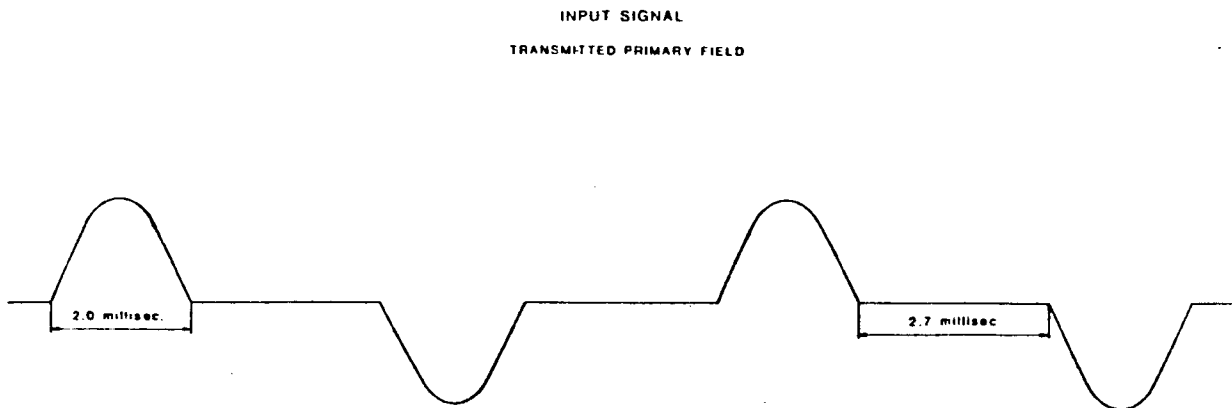


Figure A1

RECEIVER SPECIFICATIONS

Sample	Gate	Windows (centre positions)	Widths
	CH 1	340 sec	200 sec
	CH 2	540	200
	CH 3	840	400
	CH 4	1240	400
	CH 5	1740	600
	CH 6	2340	600
Sample Interval			0.5 sec
Integration Time Constant			1.3 sec
Bird Position behind Aircraft (at 40 kt)			19 metres
Bird Position below Aircraft (at 40 kt)			73 metres

Receiver features: Power Monitor 50 or 60 Hz
 50 or 60 Hz and Harmonic Filter
 VLF Rejection
 Spheric Rejection (tweak) Filter

SAMPLING OF INPUT SIGNAL

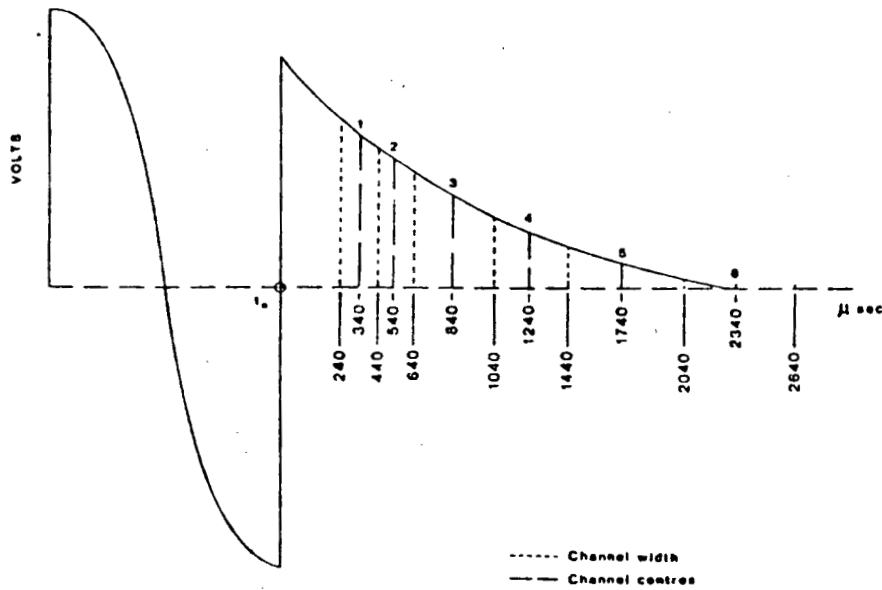


Figure A2

DATA ACQUISITION SYSTEM

Sonotek SDS 1200

9 track 800 BPI ASCII

Includes time base Intervalometer, Fiducial System

CAMERA

Geocam 75 SF

35 mm continuous strip or frame

TAPE DRIVE

Digidata Model 1139

OSCILLOSCOPE

Tektronix Model 305

ANALOG RECORDER

RMS GR-33

Heat sensitive paper (33cm)

Recording 14 Channels: 50-60 Hz Monitor, 6 INPUT Channels,
fine and coarse Magnetics, Altimeter, vertical and horizontal
timing lines and fiducial markers.

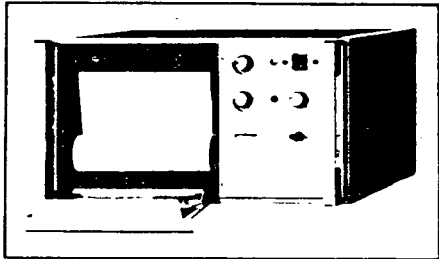
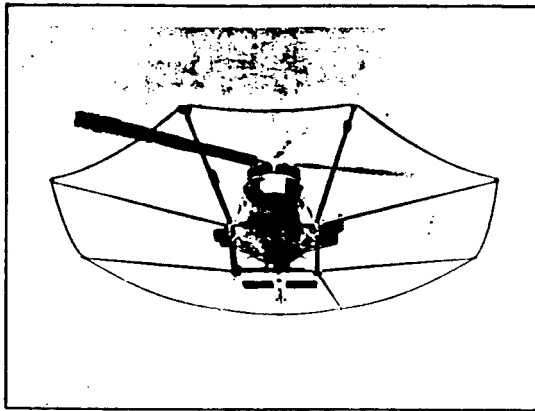
ALTIMETER

Sperry Radar Altimeter

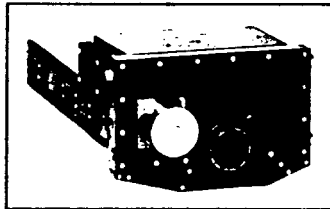
GEOMETRICS MODEL G-803 PROTON MAGNETOMETER

The airborne magnetometer is a proton free precession sensor which operates on the principle of nuclear magnetic resonance to produce a measurement of the total magnetic intensity. It has a sensitivity of 1 gamma and an operating range of 20,000 gammas to 100,000 gammas. The sensor is a solenoid type, oriented to optimize results in a low ambient magnetic field. The sensor housing is mounted on the tip of the nose boom supporting the INPUT transmitter cable loop. A 3 term compensating coil and perma-alloy strips are adjusted to counteract the effects of permanent and induced magnetic fields in the aircraft.

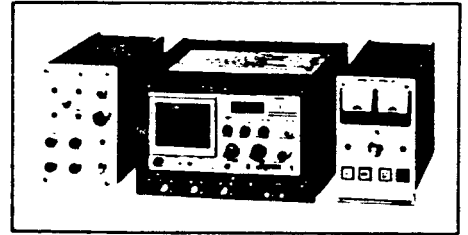
Because of the high intensity electromagnetic field produced by the INPUT transmitter, the magnetometer and INPUT results are sampled on a time share basis. The magnetometer head is energized while the transmitter is on, but the read-out is obtained during a short period when the transmitter is off. Using this technique the sensor head is energized for 0.80 seconds and subsequently the precession frequency is recorded and converted to gammas during the following 0.20 second when no current pulses are induced into the transmitter coil.



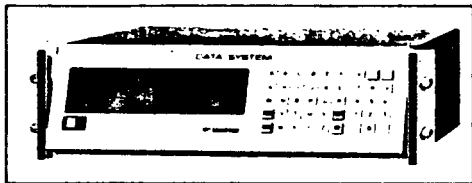
HONEYWELL ANALOGUE CHART RECORDER



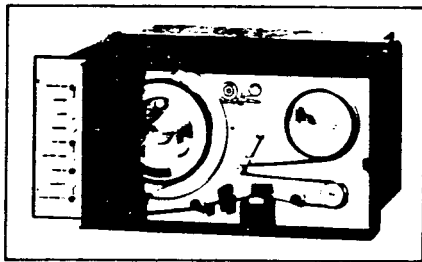
35mm TRACKING CAMERA



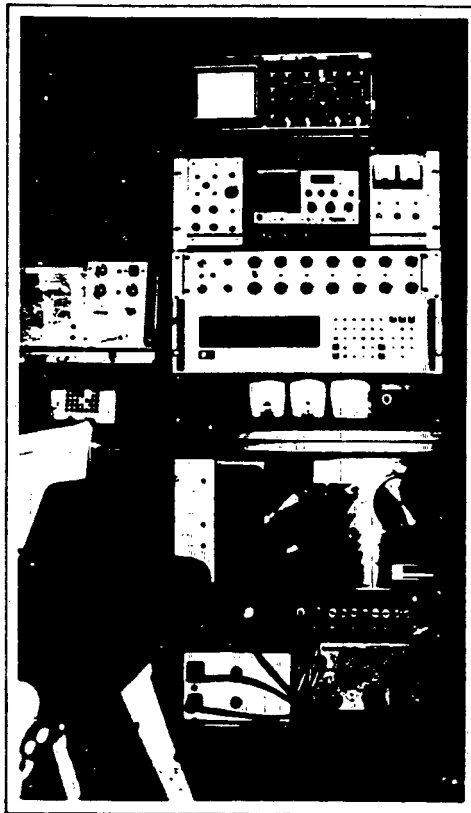
INTERFACE, OSCILLOSCOPE & T.C.U.



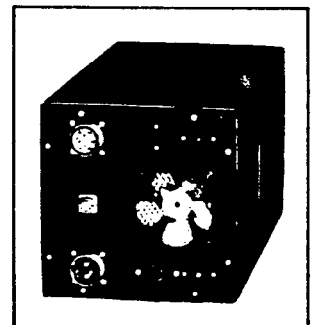
SONOTEK DATA SYSTEM



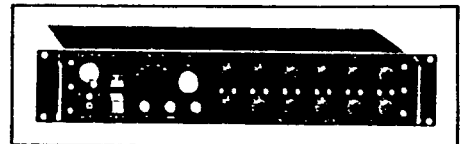
9 TRACK TAPE RECORDER



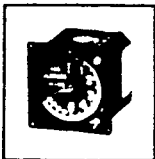
INPUT EQUIPMENT INSTALLATION



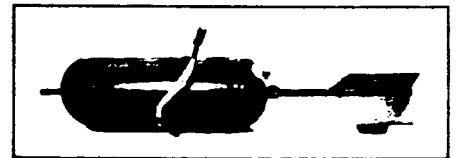
TRANSMITTER



MK VI INPUT RECEIVER



RADAR ALTIMETER



TOWED "BIRD" ASSEMBLY

QUESTOR/BARRINGER MARK VI "INPUT" SYSTEM EQUIPMENT

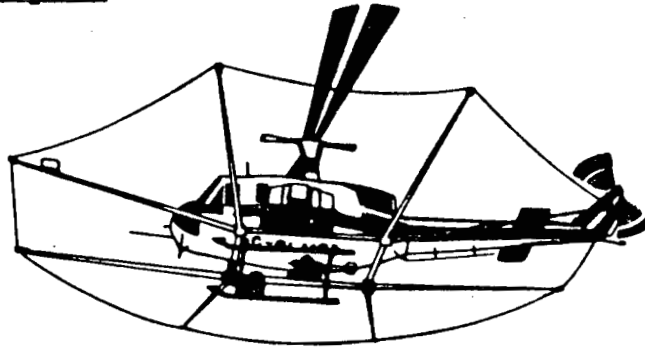
APPENDIX BThe Survey Helicopter

Figure B1

Manufacturer	Bell Helicopter Company
Type	205A-1
Canadian Registration	C-GLMC - present installation
Date of INPUT Installation	May 1982

Modifications:

- 1) Cradle and wing booms for transmitter coil mounting
- 2) Camera and altimeter mounting
- 3) Modified gasoline driven generator system

Any BELL 205-212 airframe can support the QUESTOR Helicopter INPUT system. The 205 is powered by one low maintenance turbine engine. The configuration of the helicopter provides for easy installation of equipment, which can be disassembled and crated to the survey base. Reassembly takes less than two days. These factors have proven the helicopter to be a reliable and efficient geophysical survey system in areas not suitable for fixed-wing operation.

APPENDIX C

INPUT System Characteristics

a) Geometry

The INPUT system, a time domain airborne electromagnetic system, has the transmitter loop located around the helicopter airframe while the receiver, referred to as the 'bird', typically is towed 19 metres behind and 73 metres below the helicopter at a survey airspeed of 40 knots. The actual spatial position of the bird is dependent on the airspeed of the survey helicopter, as can be seen in Figure C1.

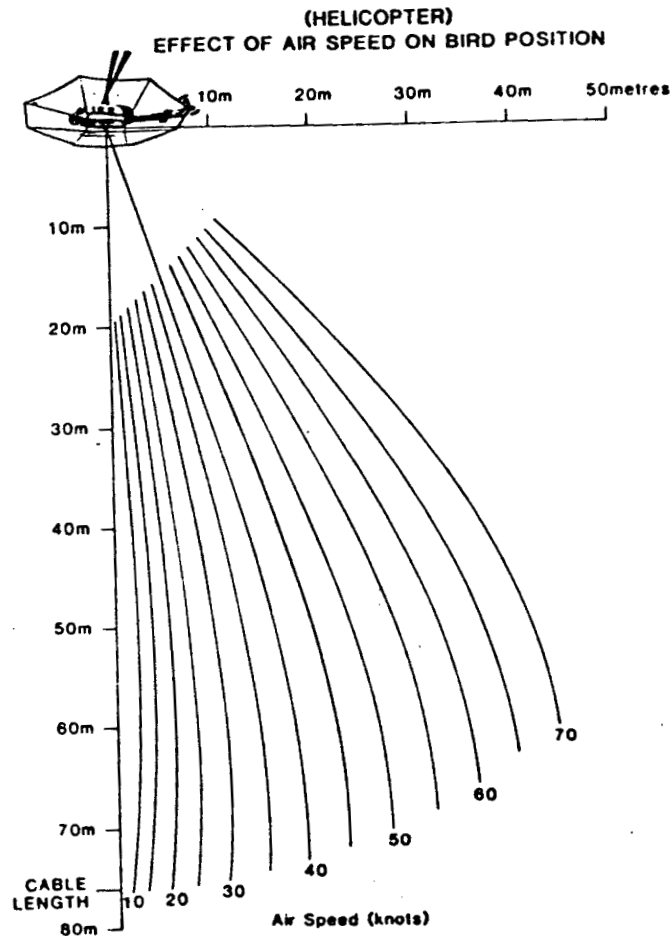


Figure C1

b) The Lag Factor

The bird's spatial position along with the time constant of the system introduces a lag factor (Figure C2) or shift of the response past the actual conductor axis in the direction of the flight line. This is due to fiducial markers being generated and imprinted on the film in real time and then merged with E.M. data which has been delayed due to the two aforementioned parameters. This lag factor necessitates that the receiver response be normalized back to the helicopter's position for the map compilation process. The lag factor can be calculated by considering it in terms of time, plus the elapsed distance of the proposed shift and is given by:

$$\text{Lag (seconds)} = \text{time constant} + \frac{\text{bird lag (metres)}}{\text{ground speed (metres/sec)}}$$

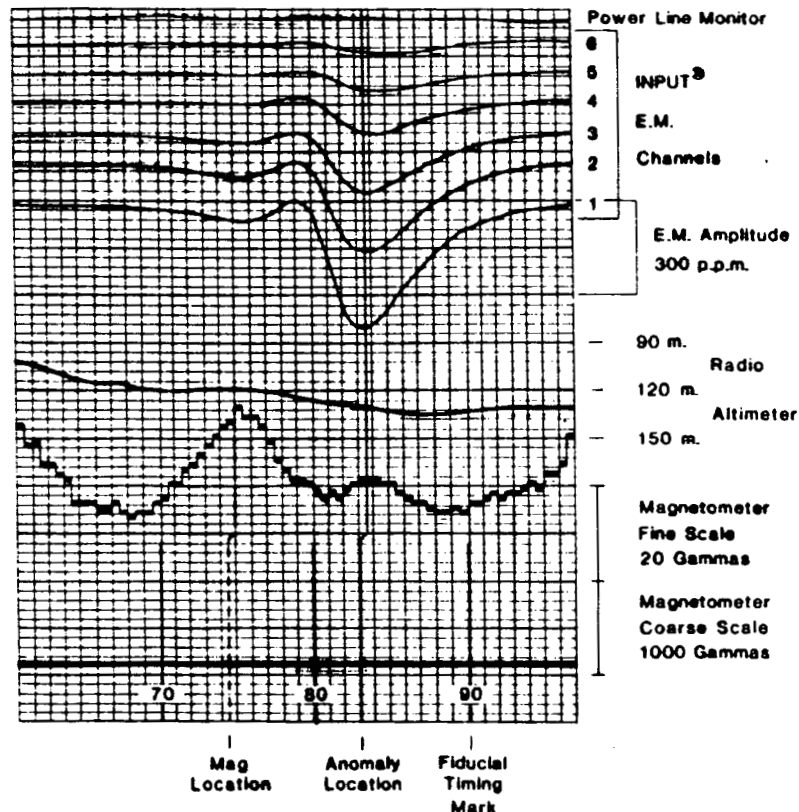


Figure C2

The time constant introduces a 1.3 second lag while, at an aircraft velocity of 40 kt., the 'bird' lag is 1 second. The total lag factor which is to be applied to the INPUT E.M. data at 40 kts. is 2.3 seconds. It must be noted that these two parameters vary within a small range dependent on the helicopter velocity, though they are applied as constants for consistency. As such, the removal of this lag factor will not necessarily position the anomalies in a straight line over the real conductor axis. The offset of a conductor response peak is a function of the system and conductor geometry as well as conductivity.

The magnetic data has a 1.0 second lag factor introduced relative to the real time fiducial positions. This factor is software controlled with the magnetic value recorded relative to the leading edge (left end) of each step 'bar', for both the fine and coarse scales. For example, a magnetic value positioned at fiducial 10.00 on the records would be shifted to fiducial 9.95 along the flight path.

A lag factor of 2 seconds (0.1 fiducial) is introduced to correct 50-60 Hz monitor for the effects of bird position and signal processing. In cases where a 50-60 Hz signal is induced in along formational conductor, a 50-60 Hz secondary electromagnetic transient may be detected as much as 5 km. from the direct source over the conductive horizon.

The altimeter data has no lag introduced as it is recorded in real time relative to the fiducial markings.

c) Calibration

The major advance made during the transition from the INPUT MK V to the INPUT MK VI has been the ability to calibrate the equipment accurately and consistently. Field tests at established test sites are carried out on an average of once every 6 months to check the consistency of the INPUT installations available from QUESTOR.

To calibrate the equipment for a survey operation the following tests are used:

- 1) "ZERO" the digital and record background E.M. levels;
- 2) magnetometer scale calibrations;
- 3) altimeter calibration;
- 4) calibration of INPUT receiver gain;
- 5) aircraft compensation;
- 6) record background E.M. levels at 600 m.;
- 7) survey flight;
- 8) record background E.M. levels at 600 m.
- 9) record full scale INPUT receiver gain;
- 10) record compensation drift;
- 11) terminate or repeat from step 4.

This sequence of tests may be repeated in midflight given that the duration of the flight is sufficiently long. Typically, this process is conducted every 2 hours of actual flying time and at the termination of every flight.

The background levels are recorded and then used to determine the drift that may occur in the E.M. channels during the progression of a survey flight. If drift has occurred, the

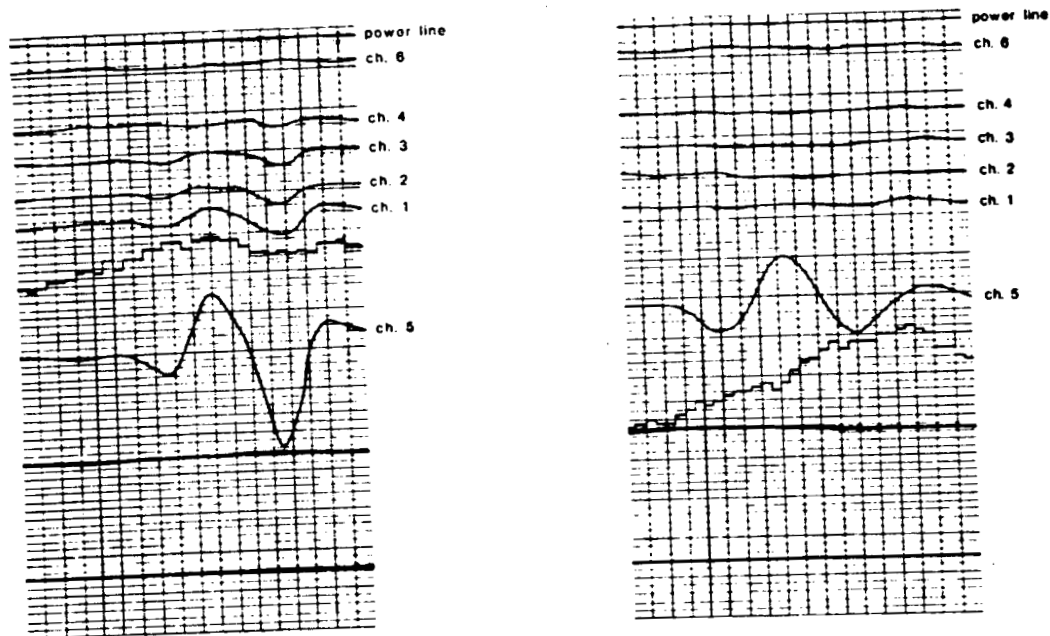
E.M. channels are brought back to a levelled position by use of the linear interpolation technique during the data processing.

The primary electromagnetic field generated by the INPUT system induces eddy currents in the frame of the helicopter. This spurious secondary field is a significant source of noise which needs to be taken account of before every survey flight is initiated.

Compensation is the technique by which the effects of this spurious secondary field are eliminated. A reference signal, which is equal in amplitude and waveform but opposite in polarity, is obtained from the primary field voltage in the receiver coil and applied to each channel of the receiver. The compensation signal is not a constant value due to coupling differences induced by 'bird' motion relative to the aircraft. The signal applied is proportional to the inverse cube of the distance between the 'bird' and aircraft. Figure C3 displays the effect of compensation.

Typically, channel 5 is selected for compensation because it is not affected by geological noise due to its sampling location in the transient and then coupling changes are induced by precipitating 'bird' motion. Phase considerations of channel 5, relative to the remaining channels, dictates whether sufficient compensation has been applied. If the remaining channels are in-phase to channel 5 during this procedure, an over-compensated situation is indicated, whereas, out-of-phase would be indicative of an under-compensation case. Normally this adjustment is carried out at an altitude of 600 metres in

order to eliminate the influence of external geological and cultural conductors.



Uncompensated

Compensated

Figure C3

The magnetometer, altimeter and INPUT receiver gain are also calibrated at the initiation of every survey flight. With the magnetometer, there are two scales, a coarse and a fine scale. The fine scale indicates a 10 gamma change for a 1 cm. change in amplitude (Figure C2). The coarse scale moves 2 mm. (or 1 division) for a 100 gamma change with full scale, 2 cm., indicating a 1000 gamma shift.

The altimeter (Figure C4), is calibrated to indicate 400 feet altitude at the seventh major division (7 cm.), read from the bottom of the analog record. This is the nominal flying

height of INPUT surveys, wherever relief and aircraft performance are not limiting factors. The eighth major division correlates with 300 feet while the sixth corresponds with 500 feet in altitude.

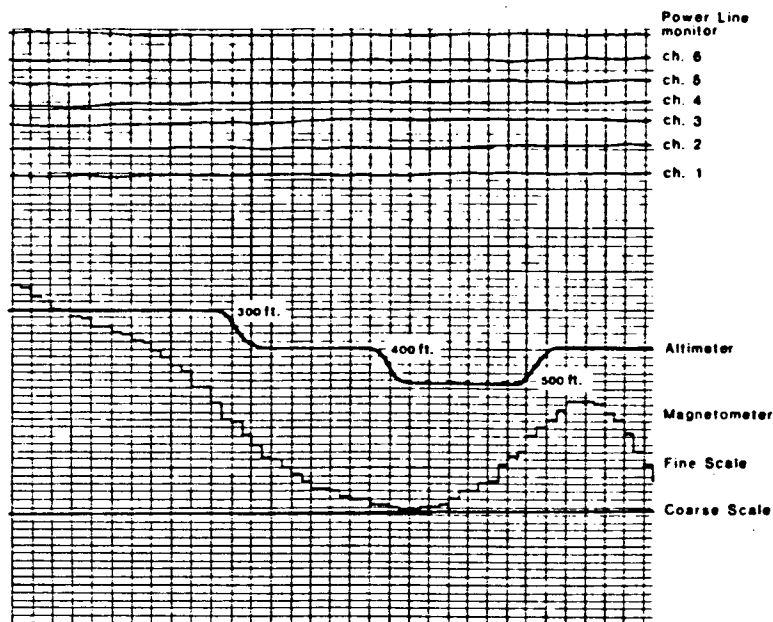


Figure C4

The INPUT receiver gain is expressed in parts per million of the primary field amplitude at the receiver coil. At the 'bird', the primary field strength is 8.5 and 8 volts peak-to-peak, for the vertical and horizontal axis coils respectively or 4.2 and 4.0 volts peak amplitude. The calibration signal introduced at the input stage of the receiver is 4.0 mV. Expressed in parts-per-million, this induces a change of:

$$\frac{4 \times 10^{-3} \times 10^6}{4.2} = 1,000 \text{ ppm (vertical coil)}$$

These calibration signals (Figure C5) cause an 8 cm. deflection of all 6 traces which translates to a sensitivity of 125 ppm/cm. for the vertical axis receiver coil system.

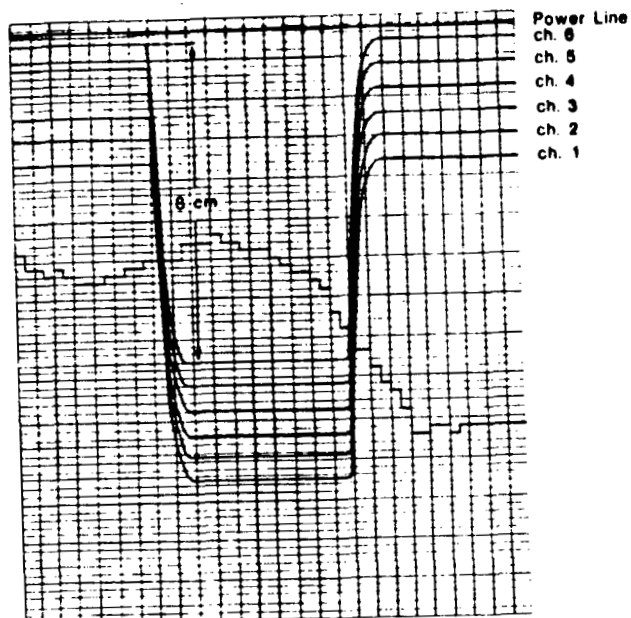


Figure C5

With the chart speed increased from the normal 0.25 cm. to 2.5 cm. per second, the time constant of the system (Figure C6), can be obtained by analysis of the exponential rise of the calibration signal for all 6 traces. The time constant, is defined as the time for the calibrated voltage to build up or decay to 63.2% of its final or initial value. A longer time constant reduces background noise but also has the effect of reducing the amplitude of the signal, especially for near surface responses.

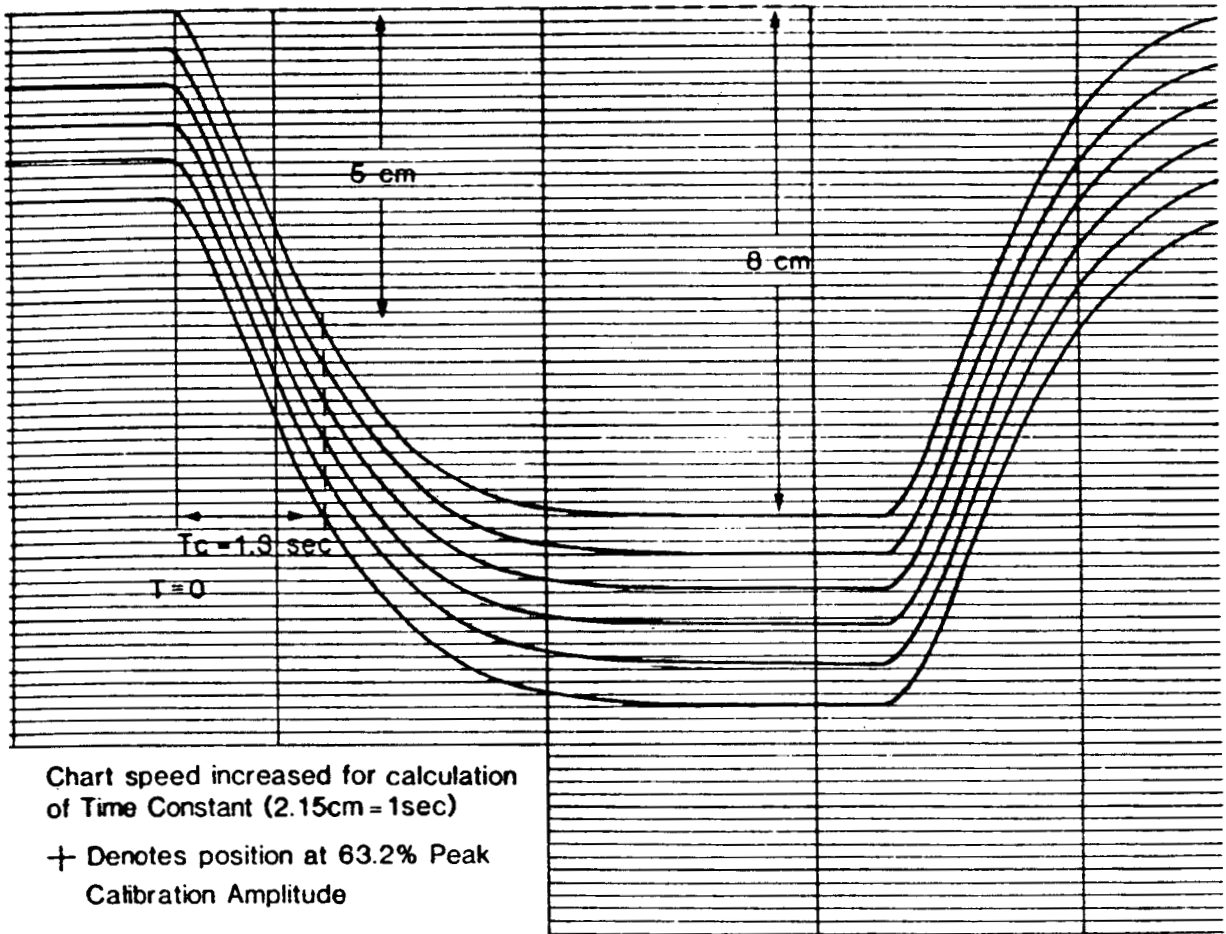


Figure C6

This trade-off indicates the importance of selecting an optimum value for the time constant. Experience and years of testing have indicated that a time constant of 1.3 second does not impede interpretation of bedrock source conductors.

d) Depth Penetration Capabilities

There are many factors which effect the depth of penetration. These factors consist of:

- 1) altitude of the helicopter above the ground;
- 2) conductivity contrast between conductor and host rock;
- 3) size and attitude of conductor;
- 4) type and conductivity of overburden present.

Of these factors, only the first parameter can be controlled. Typically, a survey altitude of 120 metres (400 feet) or less above the terrain is maintained. At this height, the helicopter INPUT MARK VI system has responded to conductors located at a depth of 200 metres (650 feet) below the surface.

APPENDIX DINPUT Data Processing

The QUESTOR designed and implemented computer software routines for automatic interactive compilation and presentation, may be applied to all QUESTOR INPUT Systems. The software is compatible with the fixed-wing MARK VI INPUT, and the helicopter MARK VI INPUT. The procedures are all common, however, separate subroutines are accessed which contain the unique parameters to each system. Although many of the routines are standard data manipulations such as error detection, editing and levelling, several innovative routines are also optionally available for the reduction of INPUT data. The flow chart on the following page (Figure D1) illustrates some of the possibilities. Software and procedures are constantly under review to take advantage of new developments and to solve interpretational problems.

a) INPUT Data Entry and Verification

During the data entry stage, the digital data range is compared to the analog records and film. The raw data may be viewed on a high-resolution video graphics screen at any desirable scale. This technique is especially helpful in the identification of background level drift and instrument problems.

b) Levelling Electromagnetic Data

Instrument drift, recognized by viewing compressed data from several hours of survey flying, is corrected by an

interactive levelling program. Although only two or three calibration sequences are normally recorded, the QUESTOR technique permits the use of multiple non-anomalous background recordings to divide a possible problematic situation into segments. All 6 INPUT channels are levelled simultaneously, yet independently. The sensitivity of the levelling process is normally better than 10 ppm on data with a peak-to-peak noise level of 30 ppm.

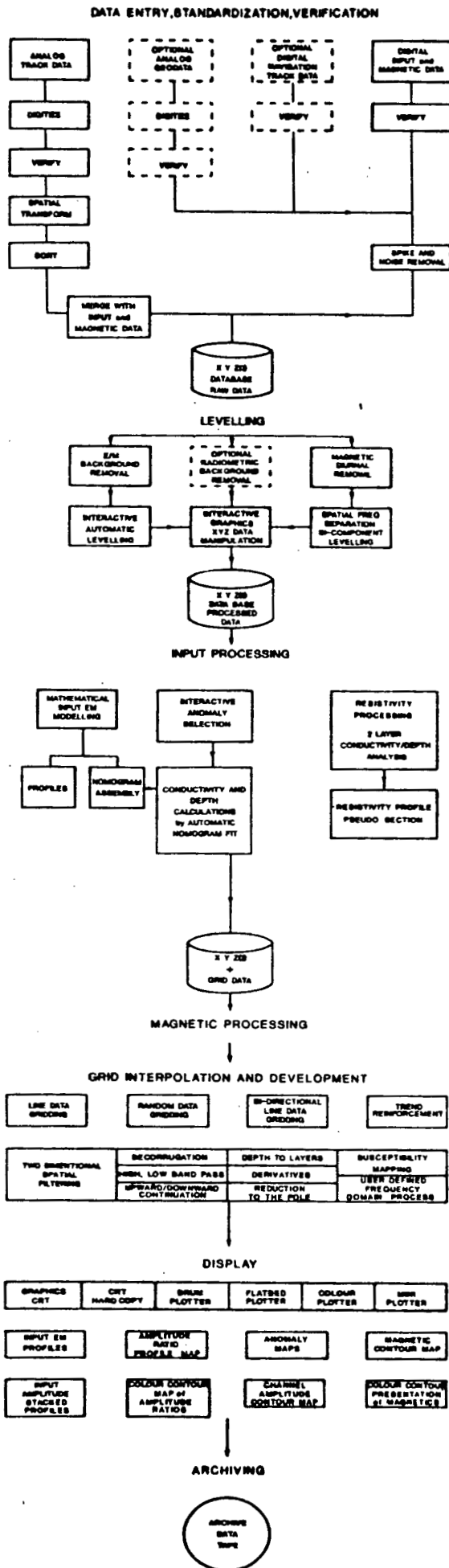
c) Data Enhancement

Normal INPUT processing does not include the filtering of electromagnetic data. The residual high frequency variations often apparent on analog INPUT data, is due almost wholly to "spherics", atmospheric static discharges. In conductive environments, spherics are apparently grounded and effectively filtered. In resistive environments, frequency spectrum analysis and subsequent FFT (Fast Fourier Transform) filters have been applied to data to reduce the noise envelope.

d) Selection of EM Anomalies

The levelled data may be viewed sequentially on a graphics screen for the selection of INPUT anomalies. Anomalies are selected by aligning a cursor to the position of the peaks. Some of the parameters of the response are manually entered during the picking of the response. These include the number of channels above background levels and the type of anomaly, e.g. cultural, bedrock, surficial, up-dip, etc.

QUESTOR INPUT DATA PROCESSING



APPENDIX EINPUT INTERPRETATION PROCEDURES

The INPUT system is dependent upon a definite resistivity contrast and is most suitable for highly conductive massive sulphides. Differentiation is possible between flat-lying surficial conductors and bedrock conductors.

The selection of anomalies is based on their characteristics and interpretation is sometimes enhanced by analyzing the magnetics. Spherics, due to atmospheric static discharges and lightning storms, are distinguishable from conductive anomalies. In the analysis of each conductor anomaly, the following parameters may be considered: anomaly shape with the conductor pattern, topography, corresponding magnetic features, anomaly decay rate, the number of channels affected, geological environment and strike direction and the interpreted dip relative to structural features.

For each anomaly selected, the following are recorded: location by fiducial, channel amplitudes in parts per million, number of channels, conductivity-thickness in siemens, corresponding magnetic association in gammas, magnetic fiducial location altitude of aircraft above ground in metres and also, the origin of the response (ie. surficial, bedrock, cultural).

Conductive responses are categorized into three main groups. These are bedrock, surficial and cultural.

Bedrock conductors can be sorted into conductive sources which are commonly encountered on INPUT surveys: massive

sulphides, graphites, serpentized peridotites and fault or shear zones. Magnetite and manganese concentrations may also yield INPUT responses in some circumstances. INPUT responses over alkalic intrusives and weathered basic volcanics have been well documented by Macnae (1979) and Palacky (1979).

Massive Sulphides

Massive sulphides occur as both syngenetic and stratified deposits and as vein infilling deposits. Nickel deposits often occur as magmatic injections of massive sulphides. Kuroko-type syngenetic copper-zinc massive sulphides usually occur at an interface of felsic intermediate rocks. In this environment, there are seldom any significant formations of carbonaceous sediments on the same horizon. Often, these deposits are overlain by a silicious zone which may contain stringers of continuous sulphides, which change to disseminated sulphides away from the main deposit. These often give a deposit the appearance of a long strike-length zone which may not fit the explorationist's target model. A careful analysis of conductivities and apparent widths (half-peak-width), will often reveal the geometry and source. Syngenetic deposits of base metal sulphides of up to 2 km strike length are not unknown, although most sizeable deposits have strike lengths between 500 and 1000 m.

The conductivity of most massive sulphide deposits may be attributed to the pyrrhotite and chalcopyrite content, as both minerals form elongated interconnected masses which are most

amenable to the induction of electromagnetic secondary fields. Pyrite normally forms cubic crystals which must be interconnected electrically in order to produce a response. Massive pyrite often produces only a moderate response which may be difficult to distinguish from graphite. The in-situ conductivity of massive sulphides, although very high for individual crystals, often falls in the range of 5 to 20 S/m.

Sulphide conductive zones are rare in nature; economic sulphides are even more scarce. Long formational sulphide zones are known, but are not common. More often, sulphide concentrations may occur within formational graphitic zones.

The geometry of many syngenetic and injected sulphide deposits may fall within broad classifications of size, conductivity and magnetization but most of these bodies are anomalous within their local geological environment. There are often changes in dip, conductivity, thickness and magnetization with respect to the regional environment. There are no rules which apply universally to massive sulphide deposits. One observation which has consistently applied to sulphide deposits is that INPUT responses (amplitude and conductivity) are roughly proportional to mineral content.

The INPUT system is capable of detecting disseminated sulphides within zones of resistivity changes. These may have low conductivities and responses will normally be restricted to channels 1 through 4. The response amplitudes will vary with the horizontal and vertical extent of the zone. Gold deposits often fall within this response classification.

The magnetic response of a sulphide deposit is the most deceiving information available to the explorationist. Although many large economic deposits have a strong direct magnetic association, some of the largest base metal deposits have no magnetic association. An isolated magnetic anomaly caused by oxidation conditions at a volcanic vent flanking a conductor, may have more significance than a body which has a uniform magnetic anomaly along its strike length. Differing geochemical environments often results in the zoning of minerals so that non-homogeneous conductivities and magnetic responses may be favourable parameters.

Graphitic Carbonaceous Conductors

Carbonaceous sediments are usually found within the sedimentary facies of Precambrian and Proterozoic greenstone belts. These represent a low energy, sedimentary environment with good bedding planes and little or no structural deformation. Graphites are often located in basins of the sub-aqueous environment, producing the same body shape as sulphide concentrations. Most often however, they form long, homogeneous planar sequences. These may have thicknesses from a metre to hundreds of metres. The recognition of graphites in this setting is normally straightforward.

Conductivities and apparent widths may be very consistent along strike. Strike lengths of tens of kilometres are common for individual horizons.

The conductivity of a graphite unit is a function of two variables:

- a) the quality and quantity of the graphite and
- b) the presence of pyrrhotite as an accessory conductive mineral

Pyrite is the most common sulphide mineral which occurs within carbonaceous beds. It does not contribute significantly to the overall conductivity as it will normally be found as disseminated crystals. Greenschist facies metamorphism will often be sufficient to convert carbonaceous sediments to graphitic beds. Likewise, pyrite will often be transformed to pyrrhotite.

Without pyrrhotite, most graphitic conductors have less than 20 S conductivity-thickness value as detected by the INPUT system or 1 to 10 S/m conductivity from ground geophysical measurements. With pyrrhotite content, there may be little difference from sulphide conductors.

It is not unusual to find local concentrations of sulphides within graphitic sediments. These may be recognized by local increases in apparent width, conductivity or as a conductor offset from the main linear trends.

Graphite has also been noted in fault and shear zones which may cross geological formations at oblique angles.

Serpentinized Peridotites

Serpentinized peridotites are very distinguishable from other anomalies. Their conductivity is low and is caused partially by magnetite. They have a fast decay rates, large amplitudes and strong magnetic correlation.

JOB NO:27H17

INPUT EM	ANOMALY	PEAK	RESPONSE	AMPLITUDES	(PPM)	TCP	ALT	MAGNETIC					
LINE	FIDUCIAL	TYPE	CHS	CH1	CH2	CH3	CH4	CH5	CH6	(S)	(M)	FIDUCIAL	VALUE
29041J	22.225		4	710	336	150	66	-	-	10	115	-	
29041K	22.743		6	1350	742	380	163	73	27	13	120	-	
29041L	23.954		6	2541	1664	1028	602	354	199	31	128	-	
29041M	24.370		6	2305	1476	918	545	339	204	34	142	-	
29041N	24.766		6	1199	786	529	343	225	144	53	141	-	
20141Y	174.720		6	1149	611	301	135	59	31	14	125	-	
20141Z	175.049		6	1203	610	282	112	45	15	11	124	-	
20141AA	175.280	W	6	1213	640	314	151	68	34	14	126	-	
20150K	195.599		4	326	199	109	51	-	-	15	139	-	
20150L	196.107		6	1421	766	387	187	81	37	14	126	-	
20150M	196.322		6	1365	694	334	144	66	26	13	124	-	
20160NN	235.930		4	825	392	179	73	-	-	10	135	-	
20160PP	236.301		6	1081	602	313	155	72	32	15	121	-	
20160RR	236.831		6	399	233	134	71	43	30	24	135	237.05	6
20160SS	237.391		2	172	36	-	-	-	-	NC	124	-	
20170J	253.296		1	30	-	-	-	-	-	NC	133	-	
20171A	256.539		6	1614	939	506	253	115	52	16	125	-	
20171B	257.292		3	443	220	104	-	-	-	10	121	257.17	10
20180KK	293.598		3	414	214	99	-	-	-	9	100	-	
20180LL	294.099		6	735	377	177	75	36	21	13	113	-	
20180MM	294.596		6	901	500	274	145	65	34	18	121	-	
20180NN	295.004		6	725	389	208	101	47	23	16	112	-	
20180PP	296.102		1	30	-	-	-	-	-	NC	133	-	
20190K	311.898		1	30	-	-	-	-	-	NC	118	-	
20190L	313.098		5	66	44	28	17	11	-	34	128	312.90	19
20190M	313.497		6	202	126	61	32	18	10	16	122	-	
20190N	314.012		6	748	445	248	121	58	29	18	131	-	
20190P	314.416		6	750	379	185	85	45	24	14	117	-	
20190R	314.993		4	425	232	117	56	-	-	12	114	-	
20190S	315.553		3	305	152	73	-	-	-	10	122	-	
20200CC	357.727		5	362	187	92	41	18	-	12	115	-	
20200DD	358.531		6	1047	540	261	123	58	30	14	121	-	
20200EE	359.158		6	1257	681	359	176	93	47	17	120	-	
20200FF	359.709		6	1277	728	376	181	87	42	15	109	-	

JOB NO:27H17

INPUT EM LINE	FIDUCIAL	ANOMALY TYPE	CHS	PEAK CH1	RESPONSE CH2	CH3	AMPLITUDES CH4	CH5	(PPM) CH6	TCP (S)	ALT (M)	MAGNETIC FIDUCIAL	VALUE
20201A	360.304		6	193	133	83	48	28	19	33	149	-	
20201B	360.590		6	204	144	82	49	32	23	29	131	-	
20201C	361.133		6	86	59	37	25	18	16	52	146	361.27	23
20201D	361.605		2	30	15	-	-	-	-	NC	137	-	
20201E	362.004		1	30	-	-	-	-	-	NC	119	-	
20201F	362.884		1	30	-	-	-	-	-	NC	131	-	
20211N	25.941		3	463	250	118	-	-	-	10	141	-	
20212A	27.493		3	282	169	94	-	-	-	14	153	-	
20212AX	27.750		4	316	184	102	62	-	-	18	151	-	
20212B	28.146		6	569	370	233	142	84	47	35	133	-	
20212C	29.196		3	30	15	5	-	-	-	6	147	-	
20212D	29.899		1	30	-	-	-	-	-	NC	142	-	
20220H	46.081		6	437	293	199	121	77	43	47	123	45.75	680
20221A	46.925		6	94	78	69	58	47	31	57	142	-	
20221B	48.549		1	30	-	-	-	-	-	NC	131	-	
20221BX	49.850		2	30	15	-	-	-	-	NC	137	-	
20221BY	50.300		4	524	215	111	58	-	-	14	130	-	
20221C	50.600		6	1559	901	506	275	150	75	21	135	-	
20221CX	50.700		6	1527	878	488	260	138	64	20	128	-	
20221D	51.044		6	1604	904	491	256	143	71	19	142	-	
20221E	51.355		6	1669	968	531	263	137	64	18	143	51.40	9
20221F	51.574		6	1359	819	451	238	131	57	19	148	-	
20231K	90.938		4	555	359	213	125	-	-	21	150	-	
20231L	91.237		3	650	402	230	-	-	-	15	147	-	
20231H	91.679		6	1439	860	480	251	132	62	19	131	-	
20232A	92.029		4	99	70	45	26	-	-	27	160	-	
20232B	92.597		2	30	15	-	-	-	-	NC	150	-	
20232C	93.009		1	30	-	-	-	-	-	NC	144	-	
20232D	94.764		4	112	59	31	14	-	-	13	117	-	
20232E	95.315		6	300	210	147	99	75	52	70	135	95.47	351
20232FX	97.050		2	129	79	-	-	-	-	NC	145	-	
20232G	97.574	W	6	752	455	257	134	68	33	20	149	-	
20232H	98.360		3	518	211	95	-	-	-	9	115	-	
20242A	112.747		3	529	204	79	-	-	-	7	126	-	
20242B	113.201		4	532	283	135	62	-	-	11	121	-	
20242C	113.593		4	563	322	179	91	-	-	15	106	-	
20242D	114.905		6	4805	2493	1244	616	321	164	15	110	114.40	200

JOB NO:27H17

LINE	INPUT EM FIDUCIAL	ANOMALY TYPE	CHS	PEAK CH1	RESPONSE CH2	CH3	AMPLITUDES (PPM) CH4 CH5 CH6			TCP (S)	ALT (M)	MAGNETIC FIDUCIAL	VALUE
20243F	118.945		3	899	422	190	-	-	-	9	138	-	
20243G	119.656	U	6	1455	864	474	239	120	56	18	131	-	
20243H	121.201		1	89	-	-	-	-	-	NC	123	-	
20243J	122.640		6	269	172	115	70	51	33	51	119	-	
20243K	123.455		6	349	218	136	84	51	26	34	124	-	
20243L	124.298		2	40	23	-	-	-	-	NC	109	-	
20243M	126.699		1	30	-	-	-	-	-	NC	137	-	
20243N	128.111		3	647	376	207	-	-	-	14	143	-	
20243P	128.321		4	840	464	247	122	-	-	14	142	-	
20243R	128.557		6	1079	603	331	168	97	50	19	137	-	
20243S	128.801		6	1035	610	335	185	97	51	20	143	129.20	6
20252A	175.499		1	38	-	-	-	-	-	NC	131	-	
20252B	175.697		1	44	-	-	-	-	-	NC	131	-	
20252C	178.210	W	6	1003	594	348	195	104	51	23	134	-	
20252D	179.124		4	1558	797	363	152	-	-	10	116	-	
20253C	183.707		5	330	99	40	27	9	-	11	117	-	
20254A	184.602		3	159	68	28	-	-	-	8	141	-	
20260A	196.427	U	6	3191	1989	1105	533	243	99	16	133	-	
20260B	196.726		4	1506	802	430	206	-	-	14	122	196.73	33
20260C	197.589		6	2645	1643	933	475	237	102	19	110	-	
20260E	200.285	U	6	3857	2530	1279	888	506	270	30	129	-	
20260F	201.522	U	5	1786	1012	525	237	112	-	14	109	-	
20260G	202.895		2	116	57	-	-	-	-	NC	120	-	
20260H	204.401		1	36	-	-	-	-	-	NC	114	-	
20260J	209.318	U	6	828	458	241	126	75	42	19	145	-	
20271S	254.902		2	30	15	-	-	-	-	NC	129	-	
20271T	256.627		3	30	17	25	-	-	-	1	145	256.30	189
20271W	257.275		3	65	28	21	-	-	-	72	123	-	
20271Y	257.729	W	3	810	281	91	-	-	-	6	130	-	
20271Z	257.948	W	4	1351	519	192	59	-	-	7	116	-	
20271AA	258.563	W	4	804	449	234	115	-	-	13	143	-	
20271BB	259.152		3	943	489	241	-	-	-	11	116	-	
20271CC	259.605	W	6	2658	1729	1052	595	334	185	27	135	-	
20271DD	259.896		6	2899	1793	1094	654	407	236	32	122	-	
20271EE	261.078		4	1990	1131	625	329	-	-	15	140	-	
20272A	263.421		6	2375	1353	716	332	159	68	15	133	-	
20272B	264.182		4	844	407	200	87	-	-	11	126	264.10	26
20272C	264.409		3	862	382	165	-	-	-	8	128	-	

JOB NO:27H17

INPUT EM	ANOMALY	PEAK	RESPONSE	AMPLITUDES	(PPH)	TCP	ALY	MAGNETIC					
LINE	FIDUCIAL	TYPE	CHS	CH1	CH2	CH3	CH4	CH5	CH6	(S)	(M)	FIDUCIAL	VALUE
20281N	100.799		2	40	22	-	-	-	-	NC	128	100.18	246
20281P	101.590		3	129	61	30	-	-	-	11	131	-	
20281R	102.015	W	4	2358	1147	496	178	-	-	9	122	-	
20281S	102.259	W	6	2310	1289	663	299	142	63	14	123	-	
20281SX	102.800		3	644	408	238	-	-	-	17	127	-	
20281T	103.403		4	1256	628	323	159	-	-	13	131	-	
20281W	103.975	W	6	4120	2524	1264	871	488	255	28	123	-	
20281Y	104.404		5	3840	2299	1265	705	397	-	22	119	-	
20281Z	105.201		6	2510	1422	787	420	246	139	21	108	-	
20281AA	105.725	W	5	2238	1385	789	412	231	-	19	130	-	
20282A	106.796		6	427	279	175	99	66	43	35	151	-	
20282B	107.225	W	6	675	434	276	155	102	57	35	125	-	
20282C	107.600		6	1135	693	383	202	111	53	20	130	-	
20282D	108.075	W	6	802	480	276	149	87	53	23	149	108.32	7
20282E	108.471	W	4	917	456	205	79	-	-	9	120	-	
20282F	108.896		2	264	141	-	-	-	-	NC	131	-	
20282G	109.497		1	128	-	-	-	-	-	NC	129	-	
20291A	76.829		5	729	420	225	115	58	-	15	149	-	
20291AX	77.150		6	847	488	279	136	74	34	19	142	-	
20291B	77.788		6	2489	1468	773	358	165	73	15	138	-	
20291C	78.230		6	2665	1546	822	391	186	83	15	124	-	
20291D	79.030		6	2444	1503	872	464	250	121	22	137	-	
20291E	79.392		6	2573	1627	943	486	258	117	21	121	-	
20291F	79.879		5	2104	1180	648	342	191	-	18	123	-	
20291G	80.619		6	4483	2553	1269	809	441	228	25	120	-	
20291H	81.448		6	4144	2553	1270	723	354	152	18	122	-	
20291J	81.915		4	1502	736	345	151	-	-	10	138	-	
20291K	83.779		6	1907	1115	594	283	135	60	15	127	-	
20291L	84.090		5	2035	1068	499	201	77	-	11	117	-	
20291M	84.899		2	73	21	-	-	-	-	NC	138	-	
20291N	86.603		1	30	-	-	-	-	-	NC	148	86.63	191
20301S	61.396		1	30	-	-	-	-	-	NC	150	-	
20301T	61.901		2	30	15	-	-	-	-	NC	118	-	
20301W	62.209		2	62	28	-	-	-	-	NC	130	-	
20301Y	62.697	W	6	2145	1139	512	193	68	17	10	119	-	
20301Z	62.966		6	1764	941	471	225	116	51	15	117	-	
20301AA	64.410		3	682	416	208	-	-	-	11	151	-	
20301BB	65.091		6	2507	1550	871	465	266	146	21	124	-	
20301CC	65.331		6	2785	1580	857	456	253	135	20	114	-	
20301DD	66.155		6	1140	663	364	192	106	55	20	110	-	
20302A	67.693		4	477	316	178	97	-	-	17	149	-	
20302B	68.113		6	788	506	282	137	70	36	18	150	-	
20302C	68.812		3	276	169	87	-	-	-	12	148	-	

JOB NO:27H17

INPUT EM	ANOMALY	PEAK	RESPONSE	AMPLITUDES	(PPM)	TCP	ALT	MAGNETIC					
LINE	FIDUCIAL	TYPE	CHS	CH1	CH2	CH3	CH4	CH5	CH6	(S)	(M)	FIDUCIAL	VALUE
20303A	69.212		2	120	71	-	-	-	-	NC	153	-	
20310A	143.197		1	30	-	-	-	-	-	NC	132	-	
20310B	143.996		4	231	132	77	35	-	-	16	122	-	
20310C	144.800		6	1705	1036	569	278	136	61	17	124	-	
20310D	145.052		6	2633	1569	820	379	183	78	15	127	-	
20310E	146.129		6	1925	1131	645	354	204	112	23	134	-	
20310F	146.399		6	2330	1393	789	422	240	126	22	122	-	
20310G	146.853		6	1649	1094	692	414	254	140	35	143	-	
20310H	147.303		6	1305	773	407	189	91	44	15	145	-	
20310J	148.296		3	282	139	76	-	-	-	14	130	-	
20310K	149.301		6	1505	814	429	214	112	56	17	121	-	
20310L	149.650		6	1730	975	474	195	76	19	12	134	-	
20310M	150.496	U	2	69	18	-	-	-	-	NC	137	-	
20322J	123.100		3	109	38	10	-	-	-	5	131	-	
20322K	123.868	W	6	1527	816	397	165	70	28	12	138	-	
20322L	124.253		6	836	461	246	126	72	38	18	129	-	
20322M	125.692		6	1433	860	457	213	110	54	16	126	-	
20322N	126.038	W	6	4303	2532	1273	1009	580	315	32	123	126.07	32
20322P	126.543	W	6	1889	1253	774	443	267	150	31	130	-	
20322R	127.206		6	794	512	321	186	115	64	33	156	-	
20322S	128.068		4	996	521	261	128	-	-	12	133	-	
20322T	128.594		4	784	425	236	121	-	-	15	139	-	
20322W	129.948		4	793	457	252	121	-	-	15	127	130.02	23
20322Y	130.298	W	6	1236	744	428	218	115	60	21	138	-	
20322Z	131.101		3	65	54	32	-	-	-	18	118	-	
20331A	61.050	U	6	2508	1451	716	296	116	41	12	115	61.17	22
20331B	61.467		4	1309	672	325	157	-	-	12	133	-	
20331C	62.293		4	721	413	237	133	-	-	18	138	-	
20331D	62.678		4	970	519	285	151	-	-	15	140	-	
20331E	63.099		4	1163	605	302	144	-	-	12	130	-	
20331F	63.800		6	827	509	302	169	103	56	26	122	-	
20331G	64.983		6	1693	1128	738	463	301	185	45	131	-	
20331H	65.766	U	6	3504	2347	1276	851	497	269	36	122	-	
20331J	66.597		4	772	396	194	89	-	-	11	131	-	
20331K	68.058		5	1693	880	404	158	57	-	10	128	-	
20331L	68.898		3	103	37	7	-	-	-	3	140	-	
20333A	72.596		1	30	-	-	-	-	-	NC	157	-	
20341R	27.999		1	30	-	-	-	-	-	NC	150	-	
20341S	29.194		2	31	20	-	-	-	-	NC	148	-	
20341T	29.870		2	147	66	-	-	-	-	NC	148	-	

JOB NO:27H17

INPUT EM LINE	FIDUCIAL	ANOMALY TYPE	CHS	PEAK CH1	RESPONSE CH2	CH3	AMPLITUDES CH4	CH5	(PPH) CH6	TCP (S)	ALT (M)	MAGNETIC FIDUCIAL	VALUE
20341W	30.596		1	89	-	-	-	-	-	NC	145	-	
20341Y	30.999		1	65	-	-	-	-	-	NC	144	-	
20341Z	32.184		3	199	73	22	-	-	-	5	140	-	
20341AA	33.062		6	1970	1007	485	213	95	38	13	111	-	
20342A	34.101	W	6	1265	694	357	170	82	37	15	126	-	
20342B	35.359	W	6	3014	2029	1264	709	400	210	32	132	-	
20342C	36.104		6	500	326	206	126	86	51	40	143	-	
20342D	37.398		6	751	412	252	150	99	63	35	117	-	
20342E	37.924		6	990	553	319	175	106	57	24	132	-	
20343A	38.602		4	176	117	75	40	-	-	24	151	-	
20343B	39.435		6	695	430	261	151	91	50	29	138	39.47	40
20343C	39.688	W	6	1827	1133	675	366	207	112	24	127	-	
20343D	40.399		3	94	73	44	-	-	-	19	122	-	
20351G	255.700		5	201	131	74	37	17	-	17	121	-	
20351H	256.224		6	1472	948	563	307	176	95	24	119	256.30	39
20351J	257.128	W	6	756	407	215	116	65	36	19	148	-	
20351K	257.688		6	453	247	144	90	64	43	34	144	-	
20351L	258.798		6	331	173	100	56	41	25	28	138	-	
20351M	259.210		6	528	297	184	112	70	42	35	121	-	
20351N	260.321	U	6	2463	1588	947	523	293	153	24	134	-	
20351P	261.318		6	1335	757	404	190	91	42	15	124	-	
20351R	261.575		5	1235	598	267	97	42	-	10	133	-	
20351S	262.100		3	238	85	32	-	-	-	7	118	-	
20351T	263.893		2	112	43	-	-	-	-	NC	131	-	
20351W	264.553		3	277	114	47	-	-	-	8	116	-	
20362J	236.445	W	6	1480	1017	613	322	149	59	21	147	-	
20362K	237.896		5	690	435	244	114	41	-	15	142	-	
20362L	239.306		1	98	-	-	-	-	-	NC	117	-	
20362M	239.785		3	683	225	71	-	-	-	6	107	-	
20362N	240.328		5	1306	659	296	112	38	-	9	129	-	
20362P	240.644		6	1320	709	368	176	84	35	15	115	-	
20362R	241.612	W	6	3440	2206	1279	756	434	234	31	124	-	
20362S	242.499		3	265	138	99	-	-	-	54	140	-	
20362T	243.799		6	203	113	70	43	29	21	40	130	-	
20362W	244.392		6	595	316	169	81	47	25	18	113	-	
20362Y	244.691		5	692	339	168	81	38	-	13	136	-	
20362Z	245.945		4	286	175	105	55	-	-	20	116	-	
20362AA	247.398		2	74	35	-	-	-	-	NC	126	-	
20362BB	247.798		1	52	-	-	-	-	-	NC	130	-	
20372C	181.697		2	30	15	-	-	-	-	NC	116	-	
20372D	181.995		2	45	36	-	-	-	-	NC	118	-	
20372E	182.891		5	275	169	98	56	25	-	20	115	-	

JOB NO:27H17

INPUT EM	ANOMALY	PEAK	RESPONSE	AMPLITUDES	(PPM)	TCP	ALT	MAGNETIC					
LINE	FIDUCIAL	TYPE	CHS	CH1	CH2	CH3	CH4	CH5	CH6	(S)	(M)	FIDUCIAL	VALUE
20372F	183.497		5	459	244	131	61	28	-	14	119	-	
20372G	184.317		5	242	142	81	53	33	-	25	133	-	
20372H	186.898		3	86	61	42	-	-	-	41	133	-	
20372J	188.135	U	6	3637	2396	1277	899	526	293	38	122	-	
20372K	188.661		6	1011	595	317	163	87	41	18	131	-	
20372L	188.985		4	1040	547	262	98	-	-	10	145	-	
20372M	190.609		2	118	45	-	-	-	-	NC	130	-	
20372N	191.753		6	878	582	332	158	75	20	16	117	-	
20373A	192.902		3	64	48	22	-	-	-	9	154	192.98	231
20373B	193.466		3	65	64	34	-	-	-	13	154	-	
20373C	195.797		1	30	-	-	-	-	-	NC	134	-	
20384B	142.630	W	5	728	316	125	50	21	-	9	121	-	
20384C	144.721	W	5	1437	706	324	130	58	-	11	120	-	
20384D	145.007		6	1326	747	391	193	95	44	16	107	-	
20384E	145.563	W	6	3152	1960	1154	635	348	182	23	114	-	
20384F	148.609		3	290	142	65	-	-	-	9	117	-	
20385A	151.396		1	30	-	-	-	-	-	NC	148	-	
20385B	152.233		4	291	142	72	38	-	-	13	132	-	
20385C	152.860		5	641	323	162	74	30	-	13	130	-	
20385D	153.197		3	543	276	124	-	-	-	9	131	-	
20385E	153.798		4	148	98	60	29	-	-	19	129	-	
20385F	155.195		1	30	-	-	-	-	-	NC	130	-	
20390B	83.695		1	30	-	-	-	-	-	NC	127	-	
20390C	84.394		4	156	101	59	29	-	-	17	127	-	
20390D	84.811		6	1136	635	303	124	45	18	12	122	84.75	13
20390E	85.033		6	1085	605	300	126	61	33	14	121	-	
20390F	85.723		5	552	262	135	62	38	-	14	136	-	
20390G	86.097		3	130	69	33	-	-	-	10	138	-	
20390H	89.100		2	46	47	-	-	-	-	NC	124	-	
20390J	89.925	U	6	1464	950	572	306	170	83	24	125	-	
20390K	90.308	U	5	976	507	248	104	43	-	12	143	-	
20390L	91.297		1	37	-	-	-	-	-	NC	127	-	
20390M	92.096		2	64	23	-	-	-	-	NC	115	-	
20391A	94.118		3	57	41	26	-	-	-	24	155	94.32	109
20402C	65.499		3	30	23	5	-	-	-	4	119	-	
20402D	65.748		1	30	-	-	-	-	-	NC	110	-	
20404A	70.662	W	6	177	126	87	54	33	18	49	149	-	
20404B	71.192		2	32	21	-	-	-	-	NC	130	72.25	101
20404C	73.536	W	6	1722	997	547	273	147	80	19	124	-	

JOB NO:27H17

INPUT EM LINE	FIDUCIAL	ANOMALY TYPE	CHS	PEAK CH1	RESPONSE CH2	CH3	AMPLITUDES (PPM) CH4 CH5 CH6			TCP (S)	ALT (M)	MAGNETIC FIDUCIAL	VALUE
20404D	73.675		6	1391	860	509	286	169	94	26	121	-	
20404E	74.844		6	1481	920	513	244	111	41	16	115	75.03	38
20404F	75.159	U	5	1384	793	387	152	54	-	11	121	-	
20404G	75.799		4	177	115	63	28	-	-	14	123	-	
20410C	11.203		4	135	78	41	17	-	-	12	116	11.50	21
20410D	11.605		5	692	360	179	72	28	-	12	121	-	
20410E	11.785		6	1275	712	364	155	66	24	13	129	-	
20410F	12.732		6	1908	1210	741	444	265	150	32	120	-	
20410G	13.698		1	30	-	-	-	-	-	NC	107	14.20	162
20410H	15.801		1	30	-	-	-	-	-	NC	126	-	
20410J	16.100		2	30	15	-	-	-	-	NC	118	-	
20410K	16.741		6	485	296	183	111	60	38	32	129	-	
20410L	17.082		5	894	460	212	88	34	-	11	141	-	
20412B	25.083		2	30	15	-	-	-	-	NC	115	-	
20422J	372.107	W	5	1275	641	287	117	45	-	10	113	-	
20422K	372.359	W	6	1097	636	348	172	84	37	17	134	-	
20422L	373.852		1	30	-	-	-	-	-	NC	121	-	
20422M	374.597		1	30	-	-	-	-	-	NC	134	-	
20422N	376.983	W	6	3917	2571	1288	1252	800	497	60	119	-	
20422T	379.700		2	66	40	-	-	-	-	NC	123	-	
20430C	311.985	U	6	3136	2209	1277	860	511	280	42	127	311.98	7
20430D	314.798		1	30	-	-	-	-	-	NC	123	-	
20430E	315.295		3	51	36	30	-	-	-	141	129	-	
20430F	315.910		4	498	320	208	122	-	-	30	139	-	
20430G	316.246		4	982	529	251	103	-	-	10	135	-	
20430H	317.201		2	56	25	-	-	-	-	NC	120	317.98	112
20442B	293.754		3	122	55	23	-	-	-	8	130	292.98	193
20442C	294.335	W	5	1236	591	248	98	39	-	9	110	-	
20442D	295.281		3	421	178	88	-	-	-	11	108	-	
20442E	296.337		2	128	72	-	-	-	-	NC	114	296.30	26
20442F	297.403		1	36	-	-	-	-	-	NC	120	297.92	74
20442G	298.419		2	106	55	-	-	-	-	NC	126	-	
20442H	299.206	W	6	3127	2051	1268	743	436	250	36	130	-	
20442L	302.224		1	56	-	-	-	-	-	NC	128	-	
20450C	233.196		2	82	16	-	-	-	-	NC	119	-	
20450F	234.997		6	1578	1015	625	346	189	93	26	121	-	
20450G	236.045		2	61	40	-	-	-	-	NC	147	-	

JOB NO:27H17

INPUT EM	ANOMALY	PEAK	RESPONSE	AMPLITUDES	(PPM)	TCP	ALT	MAGNETIC					
LINE	FIDUCIAL	TYPE	CHS	CH1	CH2	CH3	CH4	CH5	CH6	(S)	(M)	FIDUCIAL	VALUE
20450H	236.898		2	70	40	-	-	-	-	NC	122	-	
20450J	238.072		3	316	141	69	-	-	-	10	117	-	
20450K	239.149		5	1108	509	217	69	25	-	9	117	-	
20462D	217.318	W	5	1150	524	227	82	32	-	9	104	-	
20462E	217.696		5	671	357	171	82	31	-	12	114	-	
20462F	218.476		2	283	118	-	-	-	-	NC	107	218.38	54
20462G	218.917		4	495	231	96	38	-	-	9	113	218.80	16
20462H	219.601		2	92	48	-	-	-	-	NC	147	219.70	21
20462J	220.411		3	145	81	37	-	-	-	9	147	-	
20462R	224.600		1	30	-	-	-	-	-	NC	120	-	
20470B	154.098		2	30	15	-	-	-	-	NC	116	-	
20470G	157.382		5	438	255	134	57	29	-	14	135	-	
20470J	159.931		5	850	393	175	74	28	-	10	113	-	
20485G	142.917		6	1250	833	501	274	150	77	24	114	142.52	51
20490F	70.945		6	680	487	320	198	118	65	41	133	71.35	77

JOB NO:27H17

INPUT EM	ANOMALY	PEAK	RESPONSE	AMPLITUDES	(PPM)	TCP	ALT	MAGNETIC					
LINE	FIDUCIAL	TYPE	CHS	CH1	CH2	CH3	CH4	CH5	CH6	(S)	(M)	FIDUCIAL	VALUE
20681F	32.451		3	243	143	65	-	-	-	9	116	-	-
20681G	32.859	W	4	477	240	111	48	-	-	10	127	-	-
20681H	33.398		5	762	404	199	83	33	-	12	145	-	-
20681J	33.827		6	849	503	271	139	70	34	18	154	-	-
20681K	34.122		6	685	429	248	136	73	40	23	152	-	-
20681L	34.862		5	258	174	110	62	38	-	29	139	-	-

LINE NO.	FIDUCIAL	MAP	UTM CO-ORDINATES	
			EASTING	NORTHING
29041	23.0	2	106963.	132412.
29041	23.7	2	107066.	131923.
29041	24.8	2	107092.	131120.
29041	27.3	2	106961.	129763.
29041	28.5	2	106817.	128912.
20150	195.8	2	104726.	135122.
20150	196.7	2	104142.	135123.
20160	235.8	2	104175.	135020.
20160	236.7	2	104730.	134931.
20170	254.9	2	104488.	134678.
20171	256.0	2	104653.	134755.
20171	256.5	2	104301.	134780.
20171	257.3	2	103712.	134785.
20180	293.8	2	103950.	134682.
20180	294.5	2	104397.	134591.
20180	295.7	2	104928.	134467.
20190	311.6	2	105423.	134170.
20190	313.9	2	104338.	134387.
20190	315.5	2	103182.	134459.
20200	357.8	2	103230.	134205.
20200	360.1	2	104072.	134079.
20201	360.3	2	104112.	134175.
20201	360.7	2	104333.	134110.
20211	26.1	2	103336.	134014.
20212	26.8	2	103141.	134043.
20212	28.2	2	104126.	133952.
20212	29.7	2	104813.	133884.
20212	30.7	2	105431.	133829.
20220	46.3	2	105210.	133694.
20221	46.4	2	105580.	133520.
20221	49.3	2	104606.	133630.
20221	50.6	2	104127.	133700.
20221	51.6	2	103427.	133802.
20231	91.0	2	103440.	133639.
20231	91.9	2	103903.	133543.
20232	92.0	2	103829.	133641.
20232	93.1	2	104630.	133488.
20232	97.3	2	106925.	133143.

LINE NO.	FIDUCIAL	MAP	UTM CO-ORDINATES	
			EASTING	NORTHING
20243	119.8	2	106909.	133025.
20243	126.5	2	104386.	133232.
20243	128.7	2	103508.	133459.
20251	171.0	2	103615.	133151.
20252	172.0	2	103604.	133181.
20252	172.9	2	104281.	133075.
20252	176.5	2	106331.	132921.
20252	177.9	2	106873.	132803.
20252	178.3	2	107164.	132801.
20253	184.2	2	109755.	132905.
20254	184.3	2	109762.	132895.
20260	201.3	2	107032.	132610.
20260	201.8	2	106711.	132654.
20260	208.0	2	104155.	133081.
20260	209.3	2	103554.	133065.
20271	254.5	2	103911.	132740.
20271	255.2	2	104219.	132691.
20271	258.7	2	106824.	132358.
20271	259.4	2	107382.	132316.
20271	261.1	2	108259.	132174.
20271	262.4	2	108940.	132059.
20272	262.7	2	108687.	132251.
20272	265.4	2	110276.	132146.
20281	98.8	2	104079.	132552.
20281	100.3	2	104977.	132409.
20281	101.9	2	105886.	132259.
20281	102.5	2	106336.	132191.
20281	103.4	2	107001.	132170.
20281	104.2	2	107561.	132094.
20281	105.8	2	108255.	132010.
20281	106.6	2	108620.	131974.
20282	106.1	2	108503.	131978.
20282	110.0	2	110254.	131678.
20291	75.9	2	110083.	131841.
20291	79.4	2	108264.	131946.
20291	81.0	2	107477.	131985.
20291	81.9	2	106898.	131979.
20291	83.4	2	106202.	132101.
20291	84.2	2	105809.	132134.
20291	86.3	2	104968.	132257.
20291	87.3	2	104429.	132300.

LINE NO.	FIDUCIAL	MAP	UTM CO-ORDINATES	
			EASTING	NORTHING
20301	60.5	2	104188.	132113.
20301	61.0	2	104599.	132095.
20301	64.1	2	106671.	131834.
20301	64.7	2	107145.	131820.
20301	67.0	2	108317.	131857.
20301	67.4	2	108527.	131851.
20302	67.5	2	108413.	131858.
20302	69.1	2	109294.	131757.
20303	69.2	2	109331.	131606.
20303	70.6	2	110108.	131506.
20310	146.0	2	107739.	131595.
20310	146.6	2	107246.	131660.
20310	147.1	2	106870.	131682.
20310	148.1	2	106497.	131751.
20310	148.9	2	106166.	131817.
20310	150.2	2	105312.	131825.
20310	150.9	2	104837.	131869.
20310	151.8	2	104295.	131902.
20322	122.2	2	104426.	131733.
20322	122.9	2	104976.	131611.
20322	123.5	2	105415.	131551.
20322	125.1	2	106373.	131523.
20322	126.0	2	106808.	131409.
20322	126.4	2	107138.	131394.
20322	126.9	2	107524.	131313.
20322	127.4	2	107916.	131255.
20322	128.0	2	108300.	131178.
20331	61.8	2	109111.	130892.
20331	63.7	2	107926.	131075.
20331	64.1	2	107575.	131122.
20331	65.0	2	106990.	131211.
20331	65.6	2	106708.	131232.
20331	66.9	2	106191.	131297.
20331	67.9	2	105682.	131359.
20331	68.5	2	105289.	131422.
20331	69.0	2	104982.	131470.
20331	69.7	2	104427.	131527.
20333	71.2	2	105263.	131368.
20333	72.1	2	104532.	131409.
20333	72.8	2	104015.	131507.
20336	77.6	2	104083.	131589.
20341	27.9	2	103278.	131386.
20341	29.3	2	103679.	131322.
20341	31.5	2	104543.	131258.
20341	32.4	2	105282.	131235.
20341	33.2	2	105769.	131257.

LINE NO.	FIDUCIAL	MAP	UTM CO-ORDINATES	
			EASTING	NORTHING
20342	33.5	2	105277.	131249.
20342	34.1	2	105773.	131132.
20342	35.0	2	106253.	131085.
20342	36.2	2	107121.	130973.
20342	37.0	2	107887.	130755.
20342	38.0	2	108845.	130494.
20343	38.3	2	108125.	130818.
20351	255.3	2	109953.	130418.
20351	256.2	2	109127.	130504.
20351	257.1	2	108379.	130577.
20351	257.6	2	107949.	130654.
20351	258.8	2	107112.	130795.
20351	260.7	2	105965.	130878.
20351	261.7	2	105362.	131057.
20351	262.6	2	104647.	131236.
20351	263.8	2	104026.	131260.
20351	264.3	2	103871.	131292.
20352	265.0	2	104085.	131177.
20352	265.6	2	103765.	131200.
20352	266.4	2	103388.	131243.
20362	234.9	2	102724.	131036.
20362	236.4	2	103449.	130905.
20362	238.4	2	104152.	130790.
20362	239.1	2	104664.	130785.
20362	240.2	2	105427.	130752.
20362	241.3	2	106185.	130670.
20362	242.8	2	107083.	130610.
20362	243.9	2	107937.	130501.
20362	247.3	2	109717.	130275.
20372	184.6	2	107839.	130287.
20372	185.5	2	107186.	130305.
20372	186.1	2	106865.	130313.
20372	188.9	2	105511.	130581.
20372	189.9	2	104697.	130684.
20372	190.9	2	104145.	130752.
20372	192.1	2	103487.	130829.
20373	192.6	2	104100.	130794.
20373	193.7	2	103406.	130693.
20373	195.6	2	102646.	130939.
20384	139.2	2	102342.	130702.
20384	139.9	2	102763.	130663.
20384	141.5	2	103444.	130623.
20384	142.9	2	104115.	130519.
20384	143.8	2	104717.	130491.
20384	144.8	2	105516.	130418.
20384	146.8	2	106773.	130323.
20384	147.3	2	107157.	130337.
20384	148.3	2	108006.	130144.
20384	149.0	2	108612.	130099.

LINE NO.	FIDUCIAL	MAP	UTM CO-ORDINATES	
			EASTING	NORTHING
20385	151.3	2	107561.	130145.
20385	151.9	2	108042.	130092.
20385	152.4	2	108488.	130034.
20390	83.4	2	110147.	129731.
20390	85.7	2	108214.	129886.
20390	86.3	2	107701.	129964.
20390	87.0	2	107300.	129994.
20390	88.0	2	106811.	130049.
20390	90.2	2	105505.	130138.
20390	91.2	2	104706.	130243.
20390	92.4	2	104166.	130405.
20391	92.8	2	104695.	130372.
20391	94.0	2	103968.	130309.
20392	98.4	2	102313.	130495.
20392	98.9	2	101964.	130546.
20402	61.8	2	102160.	130365.
20402	62.3	2	102447.	130344.
20402	65.7	2	104201.	130052.
20402	66.4	2	104755.	130009.
20402	67.2	2	105454.	129931.
20404	70.2	2	105402.	129975.
20404	72.4	2	107091.	129826.
20404	72.9	2	107499.	129746.
20404	73.5	2	108002.	129692.
20410	10.7	2	109801.	129293.
20410	12.3	2	108328.	129443.
20410	13.0	2	107753.	129513.
20410	13.3	2	107494.	129537.
20410	13.9	2	107166.	129567.
20410	14.6	2	106860.	129590.
20410	14.9	2	106646.	129640.
20410	16.9	2	105453.	129739.
20410	17.9	2	104647.	129865.
20410	18.7	2	104223.	129886.
20411	19.6	2	104286.	129832.
20412	24.9	2	102127.	130079.
20422	367.1	2	102256.	129952.
20422	371.4	2	104667.	129670.
20422	372.3	2	105413.	129562.
20422	373.7	2	105892.	129483.
20422	374.6	2	106419.	129428.
20422	375.2	2	106824.	129392.
20422	375.7	2	107155.	129349.
20422	376.4	2	107616.	129326.
20422	377.0	2	108012.	129266.
20422	377.6	2	108419.	129202.

LINE NO.	FIDUCIAL	MAP	UTM CO-ORDINATES	
			EASTING	NORTHING
20422	379.8	2	109612.	129095.
20430	309.6	2	110067.	128860.
20430	309.9	2	109791.	128913.
20430	310.4	2	109298.	128985.
20430	311.3	2	108502.	129085.
20430	311.9	2	107965.	129110.
20430	312.4	2	107593.	129129.
20430	313.0	2	107117.	129184.
20430	313.7	2	106663.	129241.
20430	314.3	2	106390.	129320.
20430	315.3	2	105904.	129411.
20430	316.0	2	105400.	129449.
20430	316.9	2	104643.	129487.
20431	323.4	2	102183.	129835.
20442	294.8	2	105409.	129108.
20442	295.7	2	105854.	129099.
20442	296.7	2	106237.	129033.
20442	297.5	2	106725.	128999.
20442	297.9	2	107039.	128964.
20442	298.5	2	107425.	128920.
20442	299.2	2	107958.	128842.
20442	302.6	2	109972.	128449.
20450	233.2	2	109558.	128581.
20450	235.0	2	107941.	128702.
20450	236.6	2	106607.	128818.
20450	237.5	2	106120.	128865.
20450	238.1	2	105731.	128947.
20450	238.6	2	105420.	128971.
20462	217.6	2	105186.	128796.
20462	218.4	2	105704.	128765.
20462	219.9	2	106820.	128653.
20462	220.7	2	107402.	128578.
20462	224.4	2	109777.	128249.
20470	153.9	2	110024.	128123.
20470	157.6	2	106753.	128446.
20470	158.6	2	105947.	128548.
20470	159.1	2	105642.	128596.
20470	159.5	2	105283.	128639.
20485	140.6	2	105253.	128368.
20485	142.9	2	106986.	128159.
20490	71.0	2	106870.	128042.

LINE NO.	FIDUCIAL	MAP	UTM CO-ORDINATES	
			EASTING	NORTHING
29020	275.7	2	99638.	125939.
20611	268.6	2	99967.	126289.
20611	269.4	2	99541.	126376.
20621	237.3	2	99836.	126199.
20621	238.8	2	100987.	126001.
20622	239.8	2	101134.	126033.
20622	240.0	2	101306.	126006.
20631	185.3	2	101832.	125782.
20631	186.9	2	101018.	125899.
20631	189.5	2	99623.	126054.
20641	156.5	2	99817.	125810.
20641	158.0	2	100926.	125716.
20641	159.4	2	101595.	125564.
20650	116.7	2	101401.	125407.
20650	117.5	2	100758.	125514.
20650	119.4	2	99779.	125709.
20660	94.9	2	100132.	125370.
20660	96.0	2	100837.	125316.
20660	97.3	2	101686.	125122.
20670	46.2	2	102208.	124930.
20670	47.9	2	100991.	125087.
20670	49.1	2	100123.	125177.
20681	33.1	2	101671.	124691.
20681	35.0	2	102554.	124677.



INPUT® PEAK RESPONSE SYMBOLS 2ms PULSE

SURFICIAL RESPONSE	UP-DIP PEAK RESPONSE	BEDROCK RESPONSE	DECAY INTERVAL CLASSIFICATION
⊙	⊙	⊙	1 Channel (300 microseconds)
⊙	⊙	⊙	2 Channel (500 microseconds)
⊙	⊙	⊙	3 Channel (800 microseconds)
⊙	⊙	⊙	4 Channel (1200 microseconds)
⊙	⊙	⊙	5 Channel (1700 microseconds)
⊙	⊙	⊙	6 Channel (2300 microseconds)
⊙	⊙	⊙	Culture Response
⊙	⊙	⊙	Associated Magnetic Response
⊙	⊙	⊙	Anomaly Letter
⊙	⊙	⊙	Poorly Defined Response
⊙	⊙	⊙	Apparent Conductivity-Width (General) (N.C. - No Calculation)
⊙	⊙	⊙	CR. 2 Amplitude (p.p.m.)

MAGNETIC CONTOURS

—	10 Gamma Contour Line
—	50 Gamma Contour Line
—	250 Gamma Contour Line

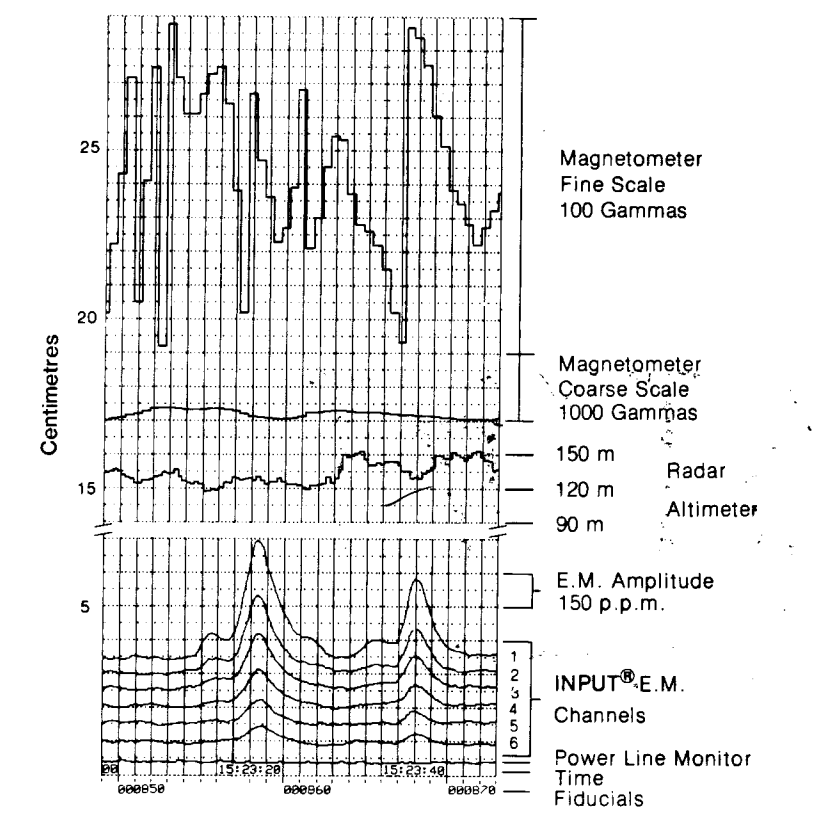
GEOLOGICAL BRANCH ASSESSMENT REPORT

14,195
1 Gamma Contour Interval

INTERPRETATION

—	20 Conductor Axis, with reference number (good definition)	○	20 Selected Zone, with reference number
- - -	20 Conductor Axis, with reference number (poor definition)	⊙	Conductive Zone
⊙	Vertical Conductor	⊙	Fault Zone
↗	Conductor Dip (magnitude and direction known)	↗	Channel 1 Half-Peak Width
↗	Conductor Dip (direction known)		

Representative INPUT® Magnetometer and Altimeter Recording

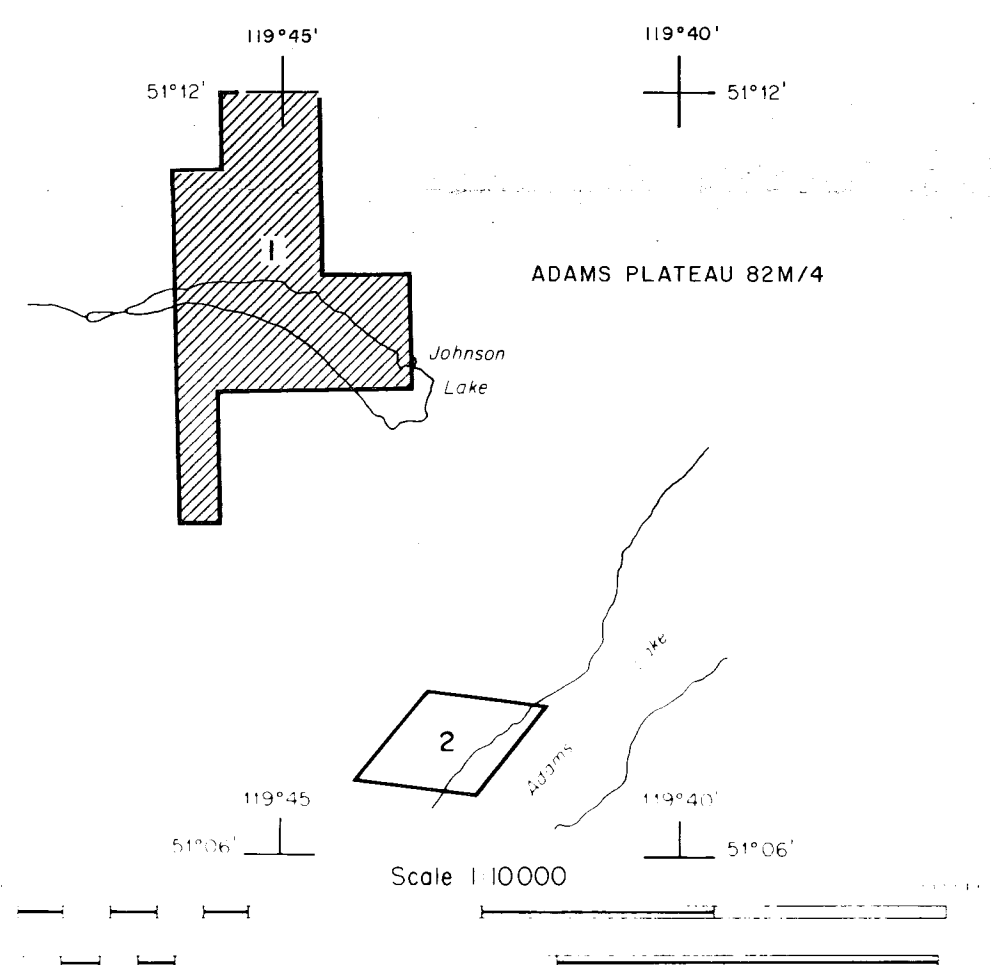


DESCRIPTIVE NOTES

The aircraft is equipped with the Barringer/Questor Mark VI INPUT® Airborne E.M. System and the Geometrics G-803 Proton Precession Magnetometer and Sonotek S50-1200 Series Data Acquisition System. The INPUT® system will respond to conductive overburden and near-surface horizontal conducting layers in addition to bedrock conductors. Discrimination of conductors is based on the rate of transient decay, magnetic correlation and the anomaly shape, together with the conductor pattern and topography.
* Registered Trade Mark of Barringer Research Limited

INTERPRETATION REFERENCES

- Becker, A., Gauvreau, C. and Collett, L.S.
1972: Scale Model Study of Time Domain Electromagnetic Response of Tabular Conductors. Canadian Mining and Metallurgical Bulletin, Volume 65, No. 725, p. 99-96.
- Dyck, A.V., Becker, A. and Collett, L.S.
1974: Surface Conductivity Mapping with the Airborne INPUT® System. Canadian Mining and Metallurgical Bulletin, Volume 67, No. 744, p. 104-109.
- Lazebny, P.G.
1973: New Developments in the INPUT® Airborne E.M. System. Canadian Mining and Metallurgical Bulletin, Volume 66, No. 732, p. 96-104.
- Nelson, Philip, H.
1973: Model Results and Field Checks for a Time Domain Airborne E.M. System. Geophysics, Volume 38, No. 5, p. 848-853.
- Plachy, G.J. and West, G.F.
1974: Computer Processing of Airborne Electromagnetic Data. Geophysical Prospecting, Volume 22, No. 3, p. 499-509.



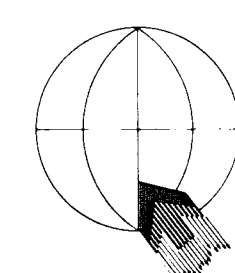
HELICOPTER MK VI INPUT® SURVEY
TOTAL MAGNETIC INTENSITY SURVEY

OMNI RESOURCES INC

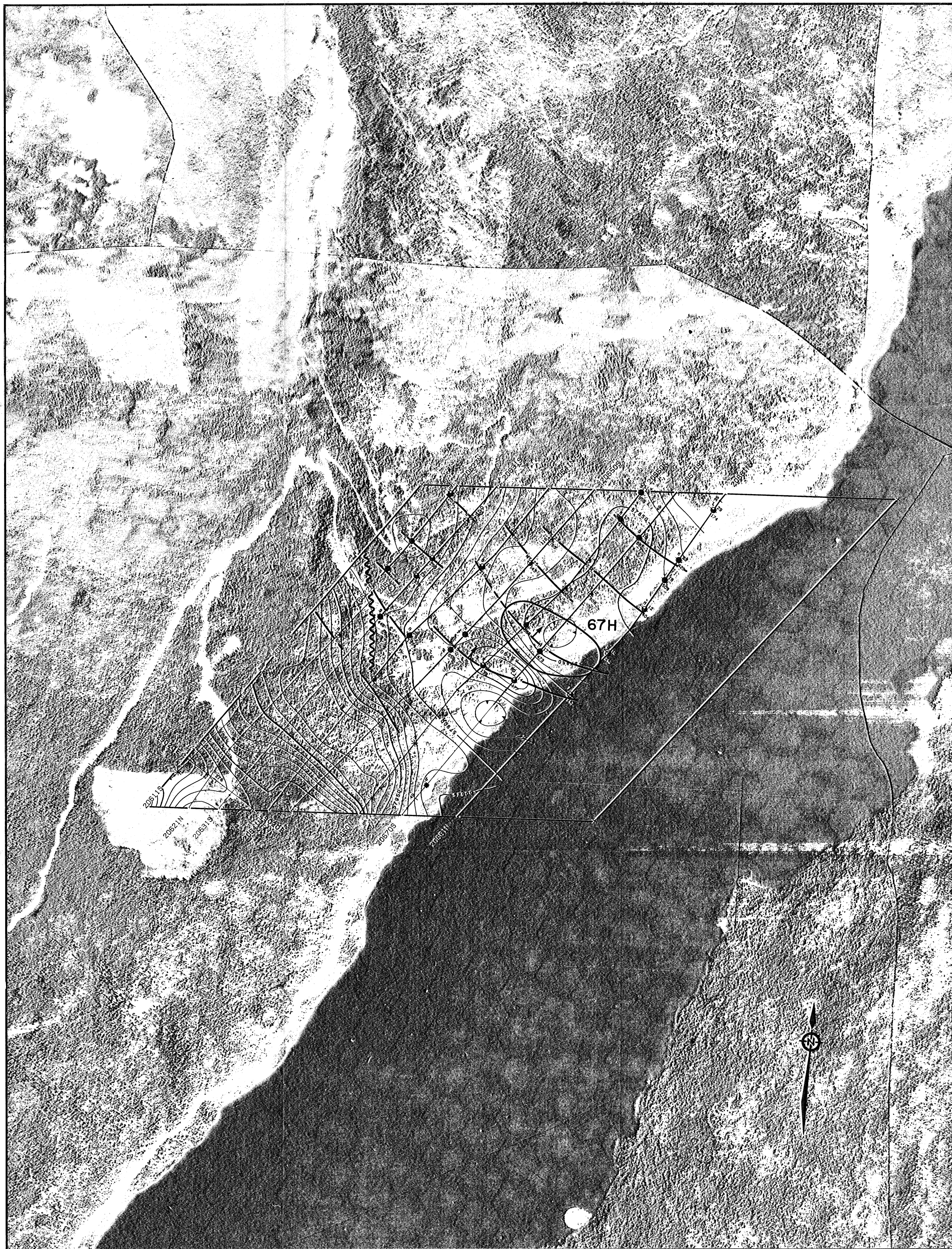
ADAMS LAKE AREA

Province of BRITISH COLUMBIA

FILE NO.	SHEET NO.	DATE	COMPILED BY
27H17C	1 of 2	June 1984	Questor Surveys Limited



Questor Surveys Limited
Mississauga Ontario Canada



INPUT® PEAK RESPONSE SYMBOLS 2ms PULSE

SURFICIAL RESPONSE	UP-DIP PEAK RESPONSE	BEDROCK RESPONSE	DECAY INTERVAL CLASSIFICATION
			1 Channel (300 microseconds)
			2 Channel (500 microseconds)
			3 Channel (800 microseconds)
			4 Channel (1200 microseconds)
			5 Channel (1700 microseconds)
			6 Channel (2300 microseconds)

Culture Response
 Anomaly Letter
 Apparent Conductivity Width (gamma) (N.C. - No Calculation)

Associated Magnetic Response
 Poorly Defined Response
 Ch. 2 Amplitude (p.p.m.)

MAGNETIC CONTOURS

	10 Gamma Contour Line
	50 Gamma Contour Line
	250 Gamma Contour Line

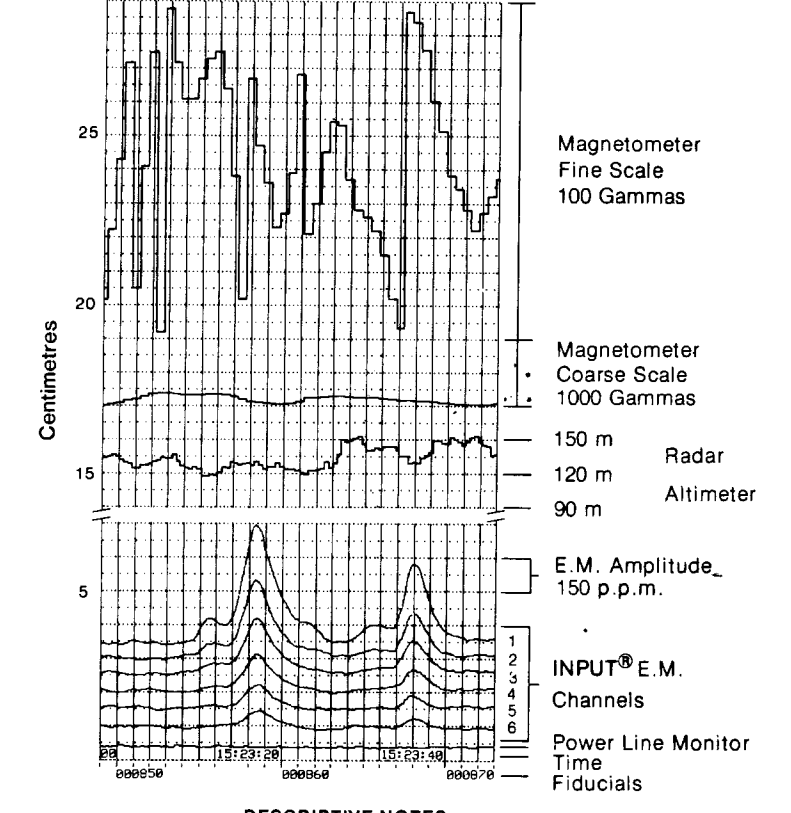
GEOLOGICAL BRANCH ASSESSMENT REPORT

14,195

INTERPRETATION

	20 Selected Zone, with reference number
	20 Conductive Zone

Representative INPUT® Magnetometer and Altimeter Recording



DESCRIPTIVE NOTES

The aircraft is equipped with the Barringer/Questor Mark VI INPUT® Airborne E.M. System and the Geometrics G-803 Proton Precession Magnetometer and Sonotek 5205-1200 Series Data Acquisition System. The INPUT® System will respond to conductive overburden and near-surface horizontal conducting layers in addition to bedrock conductors. Discrimination of conductors is based on the rate of transient decay, magnetic correlation and the anomaly shape, together with the conductor pattern and topography.

Registered Trade Mark of Barringer Research Limited

INTERPRETATION REFERENCES

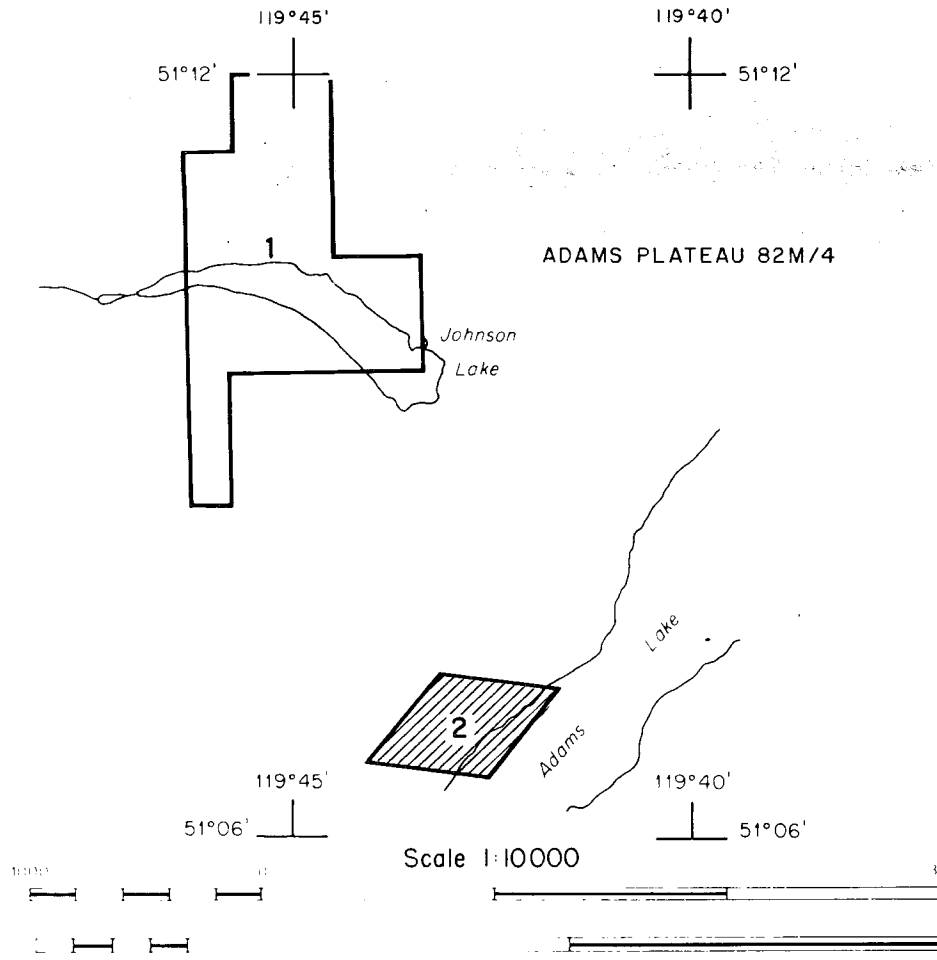
Becker, A., Gauvreau, C. and Collett, L.S.
1972. Scale Model Study of Time Domain Electromagnetic Response of Tubular Conductors. Canadian Mining and Metallurgical Bulletin, Volume 65, No. 725, p. 90-96.

Dyck, A.V., Becker, A. and Corbett, L.S.
1974. Surficial Conductivity Mapping with the Airborne INPUT® System. Canadian Mining and Metallurgical Bulletin, Volume 67, No. 744, p. 104-109.

Lazebny, P.G.
1973. New Developments in the INPUT® Airborne E.M. System. Canadian Mining and Metallurgical Bulletin, Volume 66, No. 732, p. 96-104.

Nelson, Philip, H.
1973. Model Results and Field Checks for a Time Domain Airborne E.M. System. Geophysics, Volume 38, No. 5, p. 845-853.

Palacky, G.J. and West, G.F.
1974. Computer Processing of Airborne Electromagnetic Data. Geophysical Prospecting, Volume 22, No. 3, p. 490-509.



HELICOPTER MK VI INPUT® SURVEY
TOTAL MAGNETIC INTENSITY SURVEY

OMNI RESOURCES INC

ADAMS LAKE AREA

Province of BRITISH COLUMBIA

FILE NO.	SHEET NO.	DATE	COMPILED BY
27H17C	2 of 2	June 1984	Questor Surveys Limited

Questor Surveys Limited
Mississauga Ontario Canada